Parametrization of the DO_3SE stomatal flux model for five tree species

Shubham Singh Tomar

MS13099

A dissertation submitted for the partial fulfillment of the BS-MS dual degree in Science

Indian Institute of Science Education and Research Mohali

December 2018

Certificate of Examination

This is to certify that the dissertation titled “Parametrization of the DO3SE stomatal flux model for five tree species” submitted by Mr. Shubham Singh Tomar (Reg. No. MS13099) for the partial fulfillment of BS-MS dual degree programme of the Institute, has been examined by the thesis committee duly appointed by the Institute. The committee finds the work done by the candidate satisfactory and recommends that the report is accepted.

Dr. B. Sinha (Supervisor)

Dr. V. Sinha

Dr. R. Yadav

Dated: November 30th, 2018

Declaration

The work presented in this dissertation has been carried out by me under the guidance of
Dr. Baerbel Sinha at the Indian Institute of Science Education and Research Mohali.

This work has not been submitted in part or in full for a degree, a diploma, or a fellowship to any other university or institute. Whenever contributions of others are involved, every effort is made to indicate this clearly, with due acknowledgment of collaborative research and discussions. This thesis is a bonafide record of original work done by me and all sources listed within have been detailed in the bibliography.

Mr. Shubham Singh Tomar
(Candidate)

Dated: November 30th, 2018

In my capacity as the supervisor of the candidate's project work, I certify that the above statements by the candidate are true to the best of my knowledge.

Dr. Baerbel Sinha

(Supervisor)

Acknowledgment

I would like to express my gratitude to Dr. Baerbal Sinha, my project supervisor for her kind supervision and guidance which helped me in completing my dissertation. She always guided me in right direction with correct approach regarding all project work.

I am thankful to Dr. Vinayak Sinha and Dr. Ram Yadav for providing constant valuable inputs.

I would also thank my lab members Dr. Vinod kumar, Dr. B. Prafulla, Dr. Anita, Gaurav Sharma, Pallavi, Savita, Harshita, Haseeb, Ashish, Abhishek, Tess, Jatinder, Pooja Sukhwinder, Pankaj, Aditya, Abhishek Verma, Kalik, Sanjay, Deepali, Lejish, Priya, Raman, Rishabh, Aastha, Abhilasha and Ritika for their help and support.

I would also thank Jagmeet and Bajrangi Gardner for their help.

I would also appreciate constant support from my family and friends throughout this journey.

List of Figures

List of Tables

List of Photographs

Notation (Abbreviations)

AOT40 Accumulated Ozone exposure over a Threshold of 40 ppb.

DO_3SE Deposition of Ozone for stomatal exchange (model)

g_{sto} Stomatal conductance.

POD_Y Phytotoxic ozone dose above a thresh hold of Y.

SM Soil moisture.

VPD Vapour pressure deficit.

PAR Photosynthetically active radiation.

CONTENTS

Abstract

The estimation of the ozone-induced effects on trees and setting the critical levels for ozone is necessary. Recent development in the robust stomatal ozone flux model called DO3SE model has shown great result in Europe. The multiplicative algorithm used in this model has incorporated many functions like Air temperature, VPD, Soil moisture, PAR, Ozone concentrations and plant phenological stages. And more functions like Ozone concentration, CO_2 concentration can be used for further efficiency of the model. Till now exposure based metrics like Mx, AOT40 etc. have been used in India to study any ozone-induced plant response. Here we have used another metric which is known as PODy metric. Leaf porometer was used to obtain the field data (sunlit leaf stomatal conductance). The meteorological data and the field data was taken in between May 2017 to September 2018. In this study, five tree species namely Shisham, Karanja, Babool, Amaltas, and Silk Floss tree were studied and parameterization for these environmental factors was done for DO3SE model. The boundary line parameterization of different response functions was done for each tree species. Many models are available for stomatal ozone flux modeling and no model performs well in all environment and for all species. Therefore parameterization of conductance model is necessary, in order to evaluate the performance and modify the model for better accuracy.

The study will help in progression for finding the critical level for ozone-induced effects on different tree species, the biomass loss, and identifying tree species which have a mechanism to tolerate abiotic stress like atmospheric pollutants.

Chapter 1

Introduction

1.1 Tropospheric ozone as an air pollutant

Ozone has an important role in atmospheric chemistry because it acts as the powerful oxidant. It is a major source of hydroxyl radicals (OH) (Jacob, 2000) in the lower atmosphere. While stratospheric ozone acts as a shield and filters the harmful ultraviolet radiation and protects the life on earth, on the other hand, lower atmospheric ozone (Tropospheric Ozone) is one of the most important short-lived air pollutants and affects not only human health (Shindell et al., 2012) but natural plants and crops (Fowler et al., 2009).

Moreover, studies have shown that indirect radiative forcing by ozone effects on vegetation can contribute more than direct radiative forcing (Sitch et al. 2007) as the level of tropospheric ozone has increased over the past decades (Hauglustaine et al. 1998).

1.2 Effect of environmental factors on the stomatal flux of Ozone

Post-Economic liberalization in India (after 1990s), we have witnessed an increase in tropospheric ozone levels (Kulkarni et al. 2010). Ozone and ozone-forming precursors are needed to be measured and studied, in order to quantify the damaged ozone has done as an air pollutant. The two main sources of tropospheric ozone are Transport from the stratosphere and in situ chemical production via the oxidation of hydrocarbons and CO in the presence of nitrogen oxides (Ox) (Atkinson, 2000). Plant stomata play an important role not only for plants but for atmosphere too as they are the doors for the gaseous exchange between biosphere and atmosphere. Plant phenology is comprised of all periodic events like flowering, budding etc. in the life cycle of a plant. Plant phenology plays a critical role in the stomatal flux of ozone. As in the growing

season, photosynthesis is highly active and O3 accumulation over leaves occur as stomatal aperture open for gas exchange. Moreover, plants show very less resistance to the ozone uptake (Taylor et al. 1988).

Although plants have strategies to cope up with the effects of air pollutants like ozone if the ozone level in air increases, ozone enters through a stomatal aperture or reactive oxygen species produced by ozone inside leaf tissues are not scavenged by antioxidants then visible foliar injury can be seen (Ashmore, 2005).

Various environmental factors like Air temperature, Vapor pressure deficit, Soil Moisture, Solar radiation etc. affects the plant phenological stages causing changes in stomatal flux. Similarly, tropospheric ozone shows variation in their levels with change in environmental factors. So the stomatal flux of ozone has a dynamic relationship between environmental factors, tropospheric ozone levels, and plant phenology. Optimal environment conditions are needed for the growth of the plant which varies species to species, and change in these conditions like drought, high temperature, etc. act as abiotic stress for plants. For example in Punjab two important economic species namely V. nilotica and D. sissoo are declirapidly due change in environmental factors (PUNJAB STATE ACTION PLAN 2012).

So in order to understand this dynamics and modeling stomatal flux, these environmental factors need to be incorporated into the model.

1.3 Assessment of Stomatal Ozone flux

To evaluate the role of environmental factors and their influence on the stomatal flux of plants, critical levels are found for air pollutants. Critical levels are the maximum concentration of an air pollutant above which, it can directly affect the physiology of plants. Critical levels of ozone for crops, trees, and semi-natural vegetation can be calculated either by cumulative ozone flux measurement or cumulative ozone concentrations. In order to calculate critical loads and levels, mapping manual adopted in a 2nd joint session of the EMEP Steering Body and the Working Group on Effects (2016) is used (Mills, 2017).

Earlier studies on ozone damage are shown by exposure based metrics like AOT40 which considers ambient ozone concentration for evaluation of ozone exposure. The foliar damage can only occur if ozone enters the plant through the stomatal aperture. So in order to quantify or model ozone uptake, we need to study stomatal conductance and factors controlling it. Hence flux based metric will be more biologically relevant in estimating critical levels of ozone for vegetation (Mills et al., 2011).

Currently, the DO3SE model is a widely used the model in Europe (Büker et al., 2012; Emberson et al. 2000)for the assessment of Stomatal Ozone flux. It evaluates the cumulative ozone flux, considering the influence of environmental factors causes variation in the opening and closing of stomatal aperture. The metric used in DO3SE model is called PODy (Phytotoxic O_3 Dose above a threshold flux of y) metric. To determine the accurate stomatal ozone flux for different plant species, it is divided into two sub-metrics: A) PODySPEC (Species or group specific) and B) PODyIAM (Vegetation specific).

PODySPEC is more biologically relevant for ozone risk assessment of the plant species or groups which belongs to a particular biogeographical region. Since Soil Moisture and phenology differs a lot in a large-scale area, PODyIAM doesn't account it for assessment and generally it is used for are an indicative risk assessment.

However, night time stomatal ozone fluxes can't be calculated using DO3SE model and it doesn't take count of antioxidant activity of the plant species.

Although first priority before modeling is a selection of plant species of a biogeographical region and taking accumulative data of environmental factors for the observation period like concentrations of ozone exposure to the tree canopy etc.

Following steps are needed for the modeling of stomatal ozone flux:

1 Calculation of hourly stomatal conductance of O_3 (g_{sto}).
2 Modeling hourly stomatal ozone flux (F_{st}).
3 Calculation of PODy with the data obtained from modeling (F_{st}).
4 Calculation of exceedance of flux-based critical levels.

1.3.1 Calculation of hourly stomatal conductance of O3

Most of the ozone flux model has g_{sto} (stomatal conductance) estimate at the core of their model as it gives the idea of vegetation sink capacity. The DO3SE model has incorporated four environmental factors as essential for ozone flux modeling: Photosynthetically Active Radiation (PAR), Air temperature, vapor pressure deficit (VPD) and soil moisture deficit (SM).

DO3SE model runs on a multiplicative algorithm first developed by (Jarvis, 1976) and modified by (Emberson et al. 2000), and represented by the following equation (A) :

$$g_{sto} = g_{max} \times f_{phen} \times f_{light} \times max\{f_{\min}, \ (f_{temp} \times f_{VPD} \times f_{SM})\} \qquad (A)$$

In equation (A), parameters are defined as follows:

g_{sto} is the estimated stomatal conductance and f_{min} is the fraction value of g_{min} with respect to gmax. Functions- f_{phen} is the phenology function, the f_{light} is the PAR function, f_{temp} is the temperature function, f_{vpd} is the VPD function and F_{sm} is the Soil moisture function. All these functions are relative to g_{max} which is maximum stomatal conductance observed for a species. Function f_{phen} is the modified g_{max} as a result of different phenological stages of the species over a time which is given by Julian day.These functions were defined and plotted using boundary line technique (Schmidt et al. 2000; González-Fernández et al., 2010).

1.3.2 Modelling hourly stomatal flux of O_3

For Stomatal Ozone flux modeling, alone stomatal conductance is useless if we don't calculate ozone exposure at the canopy level of the plant. The stomatal ozone flux over the projected leaf area is calculated using the following equation(B):

$$F_{st} = c(zl) \times \ g_{sto} \times \frac{D_{O3}}{D_{H20}} \times \frac{r_c}{r_b + r_c} \qquad (B)$$

Its value for Fst is given in nmol O_3 m^{-2}. Here c(zl) is the ozone concentration at the top of the canopy at the height of zl, gsto is the calculated hourly mean gsto from the model, $\frac{D_{O3}}{D_{H20}}$ is the molecular diffusivity of water vapor to that of ozone in the air, r_c is the leaf

surface resistance and r_b is the leaf quasi-laminar resistance. These leaf resitances are affected by leaf width and wind speed.

1.3.3 Calculation of POD_Y for natural ecosystems and tree

To calculate the damage done by ozone to the plant, we then find the phytotoxic ozone dose (PODy). The accumulated(hourly mean) ozone flux over the projected leaf area exceeds the ozone stomatal flux threshold of y (given in nmol m^{-2} s^{-1}) and calculated using the following equation (C):

$$POD y = \sum_{i=1}^{n} = [F_{sti} - y] \text{ for } F_{sti} > y \quad \text{(C)}$$

Here n is the number of hours of the accumulation period for ozone.

1.3.4 Calculation of exceedance of flux-based critical levels for trees

Sometimes the calculated PODy values are more than the flux-based critical value for ozone**.**

So critical level of exceedance is formed which is need to be calculated as the final step of the modeling. It is calculated using the following equation (D):

$$CL_{exceedance} = \text{PODy} - \text{critical level} \quad \text{(D)}$$

1.4 Ozone damage to natural ecosystems and trees

Ozone from lower atmosphere is settled as a dry deposition on vegetation. The tropospheric ozone has severe effects on the physiology, biochemistry, community structure, and population dynamics of forest trees (Karnosky et al., 2005). Moreover it has been seen that ozone has severe impact on tree at below ground level where it interfere with the interactions between roots with soil organisms and this change can be seen before any change on above ground level effects of ozone on trees (Hofstra et al.

1981). To evaluate the effects of ozone to natural ecosystems and tree, we have very limited studies and most of these studies are done on Europe and United States. The studies shows ozone causes foliar injury in trees and dendrochronological analysis on pine species such as *Pinus hartwegii* and *Pinus montezumae,* on sacred fir (*Abies religiosa*), and on *Prunus serotine* shows growth decline over a period of time (Alvarado R et al. 1993). In an another study on *Fagus crenata* (Japanese Beech tree), they have given a theory called ozone induced stomatal sluggishness i.e., a delay in stomatal responses to fluctuating stimuli which can affect the carbon and water balance of forests (Hoshika et al. 2014).

In the months of spring and summer, trees are highly active causing high g_{sto} which leads to more ozone uptake. Along with this high temperature and dry conditions will cause stomata to reduce g_{sto} to conserve water. Reduced dry deposition over vegetation can reduce the impact of ozone on g_{sto} (Stomatal conductance) (Emberson et al. 2013).

This shows, we have very limited knowledge about ozone damage to trees and natural ecosystem of tropical regions. India is a tropical country and there is an urgent need to study ozone-induced effects on trees as they form important part of our ecosystem. Moreover trees and natural ecosystems faces abiotic stresses like drought, floods, heat waves etc. are common in many parts of India.

Chapter 2

Materials and Methods

2.1 Site description

The Experimental sites were located at the Indian Institute of Science Education and Research Mohali (30.6650° N and 76.7300° E) i.e., there were 5 tree species as depicted in Fig. 2 and Fig. 3 respectively. All the meteorological parameters were measured at Air Quality Station (AQS Sensor), IISER Mohali. Leaf conductance measurements were taken from trees situated at 2 different sites within IISER Mohali Campus using Leaf Porometer. The distance between CAF Building and Site 1 trees was about 180m (approx.) and CAF Building and Site 2 trees were about 600m (approx.).

Figure 1 : Shows IISER Mohali Campus located on the map of India.

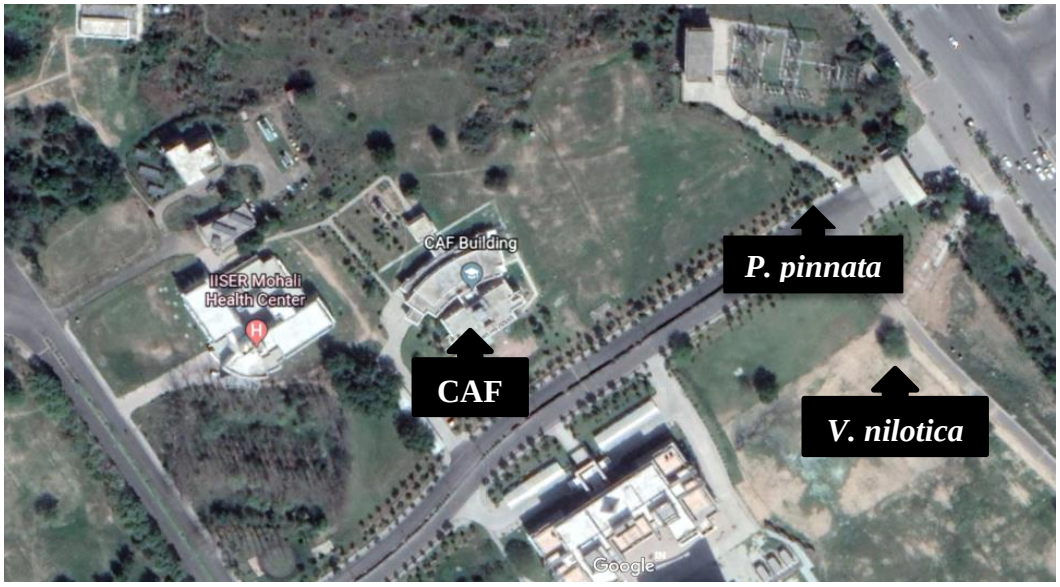

Figure 2 : Shows the Site 1 at IISER Mohali Campus where CAF buiding, *P. pinnata* (Karanja) and *V. nilotica* (Babool) tree species are located. (Credit: Google Earth)

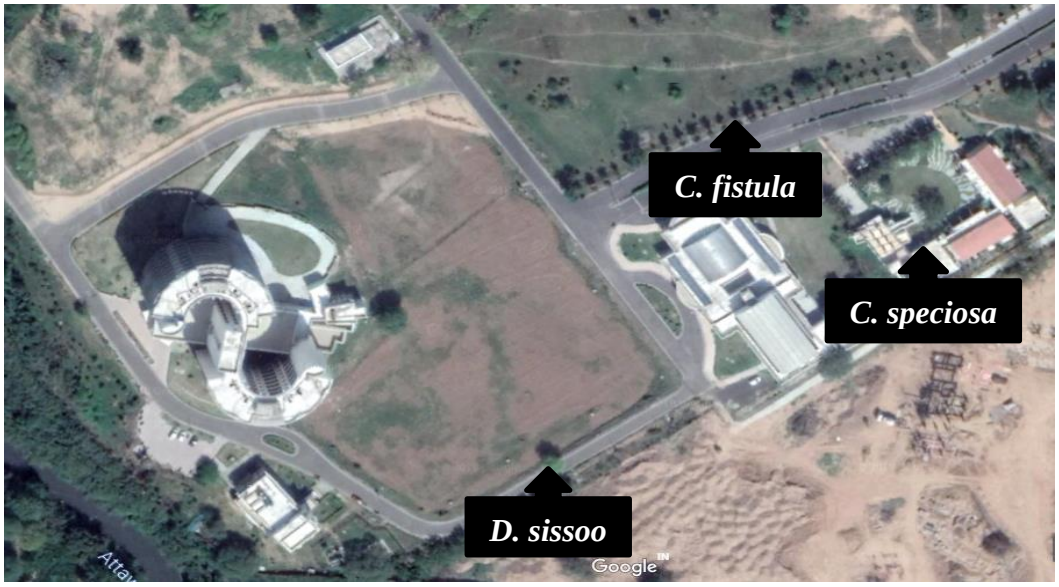

Figure 3 : Shows the Site 2 at IISER Mohali Campus where *C. fistula* (Amaltas), *C. speciosa* (Silk floss) and *D. sissoo* (Shisham) tree species are located. (Credit: Google Earth)

The region falls under the Mohali (S.A.S Nagar) district of Punjab which is bounded by Patiala and Fatehgarh Sahib district in the south-west, Ropar district in the northwest, Chandigarh, and Panchkula in the east and Ambala district of Haryana state in the south. It

is located in the foothills of the Shivalik hill ranges (Himalayan ecosystem) in the north on alluvial plains. The Soil is rich in nutrients and hence the area has large agriculture output. The soil is range from loam to silty clay which retains water and nutrients that allow good plant growth and yield.

The total geographical area of the district is 101713 ha, out of which 75010 ha is cultivable area and the main source of irrigation is through bore-wells. The forest area is about 19075 ha and the common trees are A. nilotica, A. kadamba, M. indica, D. sissoo, C. fistula etc.(PUNJAB STATE ACTION PLAN 2012).

Most of the meteorological data used are obtained from the Air Quality Station situated at top of the CAF Building (shown in Fig. 2) except Soil Moisture. Soil Moisture was obtained from Decagon EM50 sensor placed on the field.

2.1 Description of trees

2.2.1 *Dalbergia sissoo*

D. sissoo is a medium to a large deciduous tree which sheds its leaves in November and grows young leave in the first half of February, young flower buds appear with the new leaves and open in March-April. The pods are prominent by April and full-sized by July. They turn brown and the seed ripens by December or early January. It is characterized by hard rosewood with very fast growth and is commonly known as North Indian rosewood. The tropical genus Dalbergia belongs to the legume family (Fabaceae), subfamily Papilionoideae. D. sissoo is a fast-growing nitrogen-fixing tree which grows well on all kinds of well-drained soils. D. sissoo is a strong light demander from the seedling stage onwards. In India, it is valued for fodder and soil conservation, but it provides good hardwood for furniture making. It is naturally found in the Indian subcontinent and introduced in other countries. In a recent study, it has been shown that Dalbergia sissoo is moderately air pollution tolerant species with high dust removal capacity (Chaudhary & Rathore, 2018).

Isoprene is emitted by plants to increase their thermo-tolerance (Sharkey & Singsaas, 1995). A study conducted on D. sissoo in 2015 shows in the month of August and September, isoprene emissions were 32.87 ± 4.00 μg/g/h and 27.03 ± 2.70 μg/g/h

respectively (Saxena & Ghosh, 2015). And foliar emission of volatile organic compounds (VOCs) by D.sissoo was found to be 75.2 μg/g/h (Singh & Singh, 2017) using dynamic flow branch enclosure technique, initially developed by Zimmerman (1979).

Photograph 1 : *Dalbergia sissoo* tree and leaves

2.2.2 *Cassia fistula*

C. fistula is also known as golden shower tree, an evergreen, and a popular ornamental tree. The flowers appear mainly from April to July, although some trees flower as late as October, especially during dry years. It is used for medicine, fuel, timber, and tanning. It belongs to the genus Cassia and family Fabaceae. The species is native to the Indian subcontinent. Although it is an evergreen it can shed its leaves in response to pre-monsoon summer drought. The new leaves normally appear during March-July in India. The long cylindrical pods develop rapidly and ripen during December-March. They need to be chewed by jackals or dogs for new trees to germinate.

The Mean isoprene emission rate was found to be 0.2 μg/g/h (Singh & Singh, 2017). The foliar emission of volatile organic compounds (VOCs) by C. fistula was found to be 1.6 μg/g/h (Singh & Singh, 2017).

Photograph 2 : *Cassia fistula* tree and leaves

2.2.3 *Vachellia nilotica*

Vachellia nilotica is an evergreen tree with broadleaf and thorny thickets. Flowering occurs several times in a year but in the months of March to July, it occurs abundantly. Fruiting occurs in the months of June to September. Full-fledged pods can be observed in February

Photograph 3 : *Vachellia nilotica* tree and leaves

and ripening of pods occurs from April to June. Precipitation greatly affects the seeding and leafing and on the other hand, fruiting and flowering are influenced by temperature. It belongs to the genus Vachellia (formerly was under Acacia genus) family. The tree is used for various purposes like resin extraction, medicine, fodder, fuel, and tannins. Although the tree can't be leafless, leaves shed during May and June. It also forms an important

symbiotic relationship with certain soil bacteria, these bacteria form nodules on the roots and fix atmospheric nitrogen.

In scientific literature, all research groups have shown that the isoprene emission rate and the VOC emission rate for V. nilotica is below the detection limit (bdl) (Padhy & Varshney, 2005).

2.2.4 *Ceiba speciosa*

Ceiba speciosa is an ornamental deciduous tree, which is also known as the Silk Floss tree. The distinct morphological feature is its big belly trunk with thick and sharp conical prickles (spinose structures).

The tree starts shedding its leaves by mid-October and renew them in late February. The leaf fall is followed by floral bud initiation in November and mass production of showy pink flowers occur till February. Pear shaped fruits start appearing at the end of March and continue until the end of April. After blooming, pear-shaped fruits appear which have a silky floss on the seeds, hence the name. It belongs to the genus Ceiba and family Malvaceae. The silk floss tree is cultivated mostly for ornamental purposes. But people also use it to make canoes, like wood pulp, and to make paper. The bark has been used to make ropes and from vegetable oil can be obtained from seeds.

It is one of the low VOC emitter species as shown by (Varshney & Singh, 2003). However, another group reported following: The isoprene emission rate reported is 0.2 μg/g/h and total VOC emission rate is < 0.4 μg/g/h (Padhy & Varshney, 2005).

Photograph 4 : *Ceiba speciosa* tree and leaves

2.2.5 *Pongamia pinnata*

P. pinnata commonly known as Indian Beech is a medium-sized deciduous tree. Flowering generally starts after 3 to 4 years in small clusters. Leaf fall starts around December till February and flower blooms from April till June. In between leaf fall and flowering, fruiting occur from February to May. It belongs to the genus Millettia and family Fabaceae. It is drought resistant and fixes nitrogen through its root nodules. It is used for the ornamental purpose and its seed oil is used as medicine, lamp oil, insecticide etc. The Pongamia oil is also used as feedstock for first and second generation biodiesel.

It is a moderate VOC emitter, with Isoprene emission reported as 25.9 μg/g/h and total VOC emission rate as 28.0 μg/g/h (Singh & Singh, 2017).

Photograph 5 : *Pongamia pinnata* tree and leaves

2.3 Leaf Porometer and its working principle

In trees, gas exchange occurs through a tiny aperture on the leaf surface, known as Stomata. They open and close in response to sunlight and other abiotic factors like rainfall, drought etc. So they regulate water loss from plant leaves, abiotic stress and the uptake of CO_2 for

photosynthesis. Therefore, in order to study plant growth and plant physiological adaptation to environmental variables, we need to know stomatal conductance. Stomatal conductance depends on the density, size, and degree of opening of stomata on the leaf surfaces. The Gaseous exchange is governed by Fick's Law

$$E = \frac{C_L - C_a}{R_L + R_a}$$

Where, E= Evaporation (mol m^{-2} s^{-1}), C= Concentration (mol mol^{-1}), R= Resistance (m^2 s mol^{-1}), L= leaf and a= air

To measure stomatal conductance we used SC-1 Leaf Porometer from Decagon Devices. The instrument specifications included the operating environment of 5°C - 40°C and 1-100% relative humidity with a desiccant chamber with an accuracy of 10%. The aperture of the sample chamber was 6.35 mm and measurement could range from 0 to 1,000 mmol/m^2s^1 (Devices, 2016)

Working principle of SC-1 Leaf Porometer

The SC-1 Leaf Porometer measures the stomatal conductance of leaf, by placing the conductance of leaf in series with two known conductance elements. It measures the amount of water vapor difference across one of the known conductance elements (humidity sensors).

From this we get water vapor flux and using the following equation (1) we get the stomatal conductance:-

$$F_{vapour} = g_{d2}(C_1 - C_2) \quad (1)$$

where F_{vapour} is the water vapor flux, g_{d2} is the conductance across path d_2 and C values are mole fraction of vapor at both humidity sensors.

The C values are related to relative humidity by Equation (2)

$$C_i = \frac{h_r e_s(T_a)}{P_{atm}} \quad (2)$$

where h_r is relative humidity, $e_{s*}(T_a)$ is saturated vapor pressure at the temperature (T_a) and P_{atm} is the atmospheric pressure.

Saturated vapor pressure is calculated by the Tetens formula with appropriate coefficients for water vapor given in equation (3):

$$e_s(T_a)=0.611\exp\left(\frac{17.502\ T}{T+240.97}\right) \tag{3}$$

To determine the value of g_{d2}, equation (4) is used:

$$g_{d2} = \frac{\rho D_{vapour}}{d_2} \tag{4}$$

where ρ is the density of the air and

D_{vapour} is the diffusivity of the water vapor.

Placing C and g values in equation (1) we get,

$$F_{vapour} = \left[\frac{\rho D_{vapour}}{d_2}\right]\frac{1}{P_{atm}}\left[h_{r_1}e_s(T_{a_1}) - h_{r_2}e_s(T_{a_2})\right] \tag{5}$$

For g_s (stomatal conductance of leaf surface, we require some assumptions:

We assume relative humidity within leaf tissue is 1, so by equation (6)

$$C_{leaf} = \frac{e_s(T_a)}{P_{atm}} \tag{6}$$

To make flux constant between 2 nodes, we assume all conductance values are in series and temperature of the first humidity sensor is equal to the leaf temperature as sensor blockhead is made up of aluminium). So between leaf surface and first humidity sensor, F_{vapour} would be obtained by putting equation (1) = equation (4)

$$F_{vapour} = g_{s+d_1}(C_{leaf} - C_1) \tag{7}$$

And lastly, we find gs, using the rule for series conductance given in equation (8)

$$\frac{1}{g_s} = \frac{1}{g_{s+d_1}} - \frac{1}{g_{d1}} \tag{8}$$

The Leaf Porometer Function diagram below represents these measurement process.

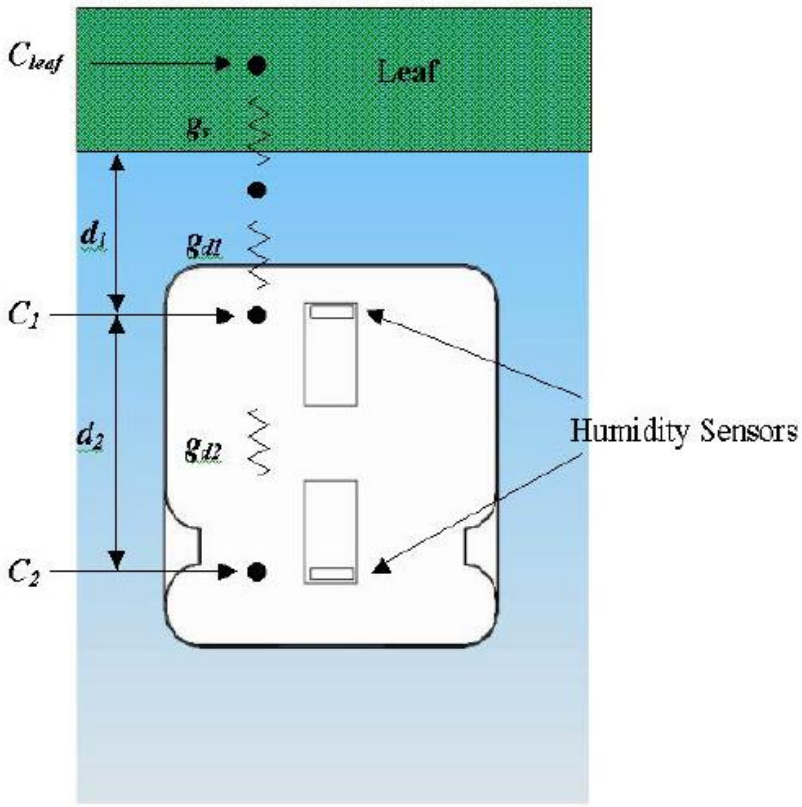

Figure 4: Function of leaf porometer (Reproduced with kind permission of the manufacturer from the instrument manual).

2.4 Manual calibration

The accuracy and precision of leaf porometer are important and for this, the two humidity sensors in the sensor head must behave in a very repeatable manner. The calibration process starts with ensuring the porometer sensor head is in thermal equilibrium with the environment and instrument time is set correctly. Since it is typical to change the desiccant each day, so we refill desiccant once in a day. The Leaf Porometer calibration apparatus consists of a plastic calibration plate with a precisely drilled hole with known conductance of 240 mmol/m^2s^1. Then we calibrate the instrument manually under field conditions by following steps:-

Step 1: Saturate filter paper with de-ionized water and place it on the calibration plate using tweezers. The paper must be wet enough to provide a 100% humidity surface, but must not be too wet.

Step 2: Then we attach the sensor head to the calibration plate, measure the conductance of filter paper and saving the data.

Step 3: Then we shake the sensor head to equilibrate the humidity inside the sensor head chamber and measure the conductance of filter paper again (5 measurements were taken for each manual calibration).

After the manual calibration was done, leaf conductance measurement could be commenced.

Graph (1) shows the calibration factor as a function of temperature. By doing the least square fitting method, we obtain a linear equation of the data set i.e., $y = mx + c$. Replacing x with temperature (°C) and m and c are constants. Then using y we can correct the calibration factor and finally correct the stomatal conductance.

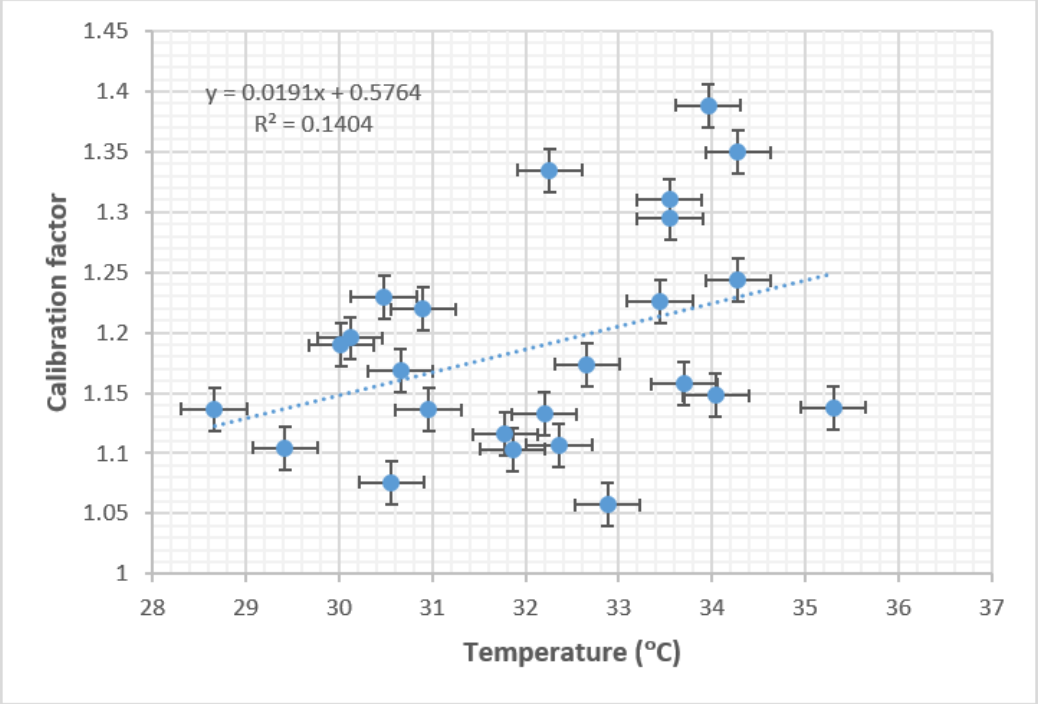

Figure 5: Calibration factor vs temperature (°C) graph

2.5 Leaf Surface selection for taking the measurements

Stomata are the portals for gas exchange between the leaf mesophyll cells and the environment. They occupy between 0.5% and 5% of the leaf epidermis. In Monocots (like Wheat) stomata are present in both upper and lower surface of the leaf while in Dicots (like tree species) stomata are present in the lower surface of the leaf. (www.pediaa.com)

Figure 6 shows the box plot between lower leaf surface conductance vs upper leaf surface conductance. The plot shows the spread of the data which has more range in case of lower leaf surface box. As the data comprised of both young and old leaf of all 5 tree species due to this variability some outliers are there in the plot as seen in case of upper leaf surface whisker. The comparison clearly shows that trees have more stomata on the lower surface of the leaf.

The young leaf of the mountain beech tree shows high photosynthesis rate in comparison to older leaf due to increased biochemical limitations (Whitehead et al. 2011).

The stomatal conductance of trees depends on many factors directly or indirectly such as, VPD (Vapor-pressure deficit), PPFD (Photosynthetic Photon Flux Density), Possibly Soil Moisture, the age of the leaf, leaf position on the plant etc.

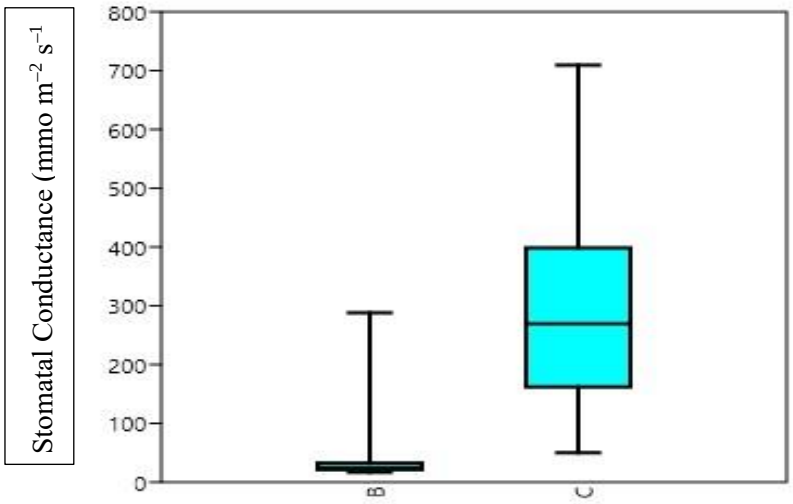

Figure 6: Box plot showing (B) upper leaf surface vs (C) lower leaf surface stomatal conductance

Chapter 3

Results and Discussion

3.1 Typical meteorological conditions

The climate of the region shows the general trend of meteorological conditions over a period of time (seasons). The physiological changes in the plant's life cycle are also decided by the change in these meteorological parameters.

Figure (7), (8), (9) and (10) shows observation time: May (2017-October 2017) meteorological data acquired from AQS sensor and Decagon sensor placed at IISER Mohali. The data acquired from the same sensors for past and following years shown here, except for some minor changing conditions due to local factors and long-range atmospheric transports.

Temperature and Wind speed shows a decreasing trend from May to October. There are few spikes (increase) near the onset and post-monsoon season as shown in Figure (7).

During summer high temperature supports increase photosynthesis rate and due to high temperature low pressure is developed causing high wind speed. Higher stomatal ozone flux is observed during this time.

Ozone tolerant plant species have very less effect of an increase in temperature and wind speed while ozone-sensitive plant species shut down their stomata in response to an increase in wind speed and temperature.

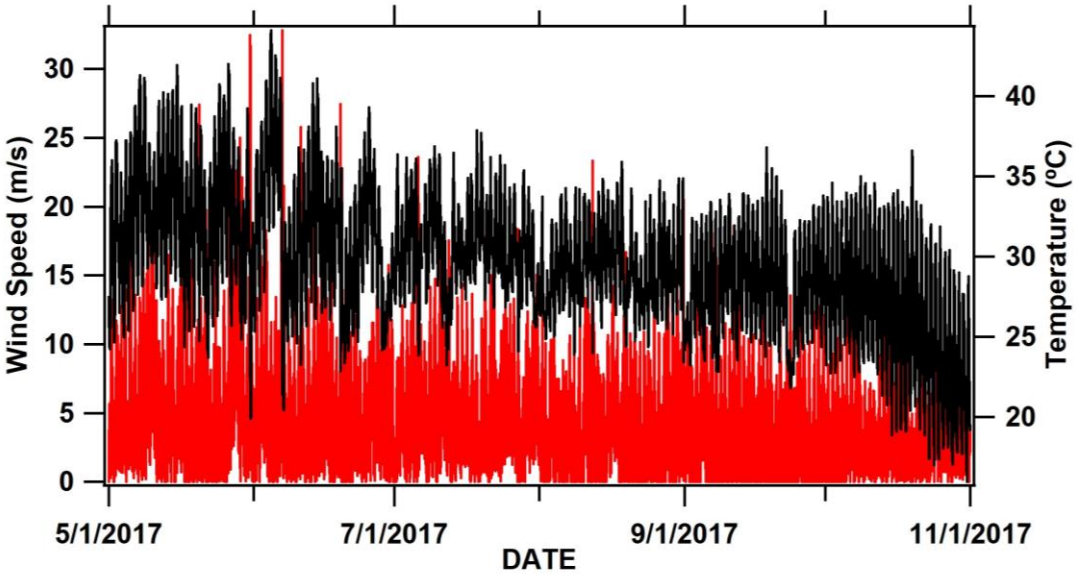

Figure 7: Temperature vs Wind Speed (Met-Data 2017) acquired from AQS sensor

Warmer air tends to hold more water vapor in the air. Figure (8) shows soil moisture decreases and VPD increases with the subsequent season. High Relative humidity causes low VPD as seen in summer. The drying capacity of air increases in summer, plants adjust their stomata and water loss. Due to this plant growth and yields are decreased.

With the increase in temperature solar radiation is also increased. Figure (9) shows a decreasing trend of solar radiation from summer to winter. PAR, which is a visible part of solar radiation and essentially used for photosynthesis by plant. PAR shows similar trend as of the total solar radiation.

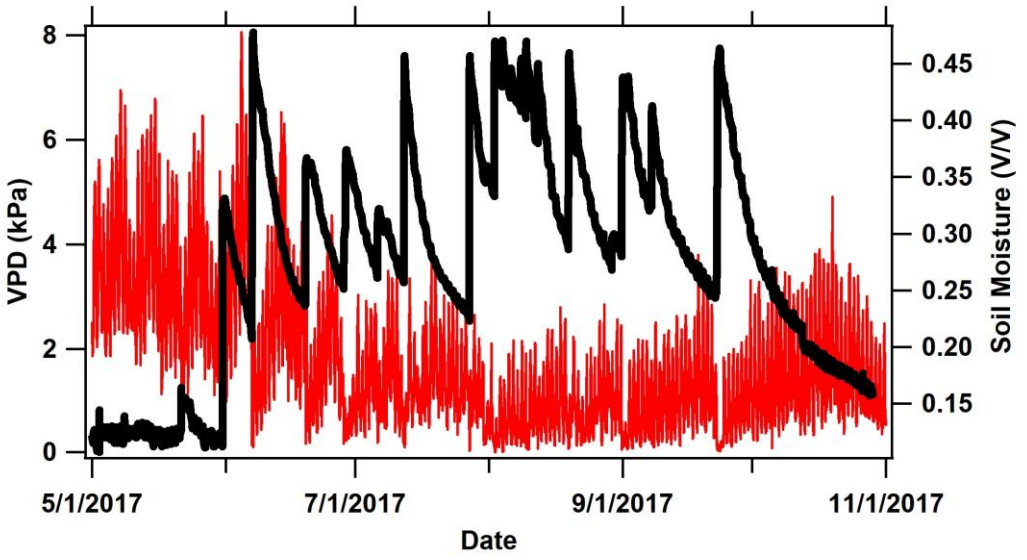

Figure 9: VPD vs Soil Moisture (Met-Data 2017) acquired from AQS sensor and Decagon sensor respectively

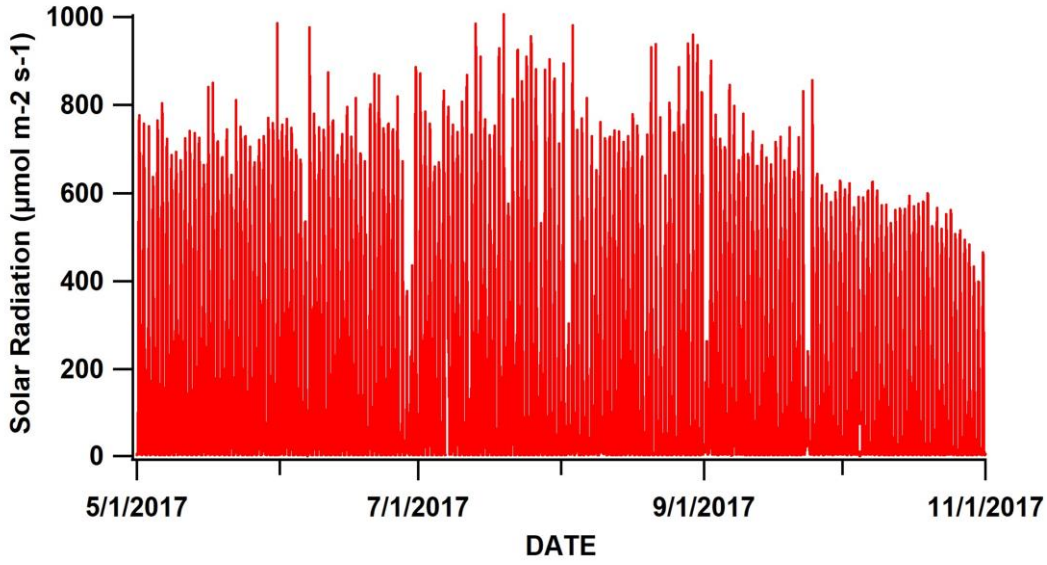

Figure 8: Solar Radiation (Met-Data 2017) acquired from AQS sensor

The Average Ozone and CO_2 concentrations trend are shown in Figure (10), which indicates CO_2 levels are higher in summer and post-monsoon season due to several

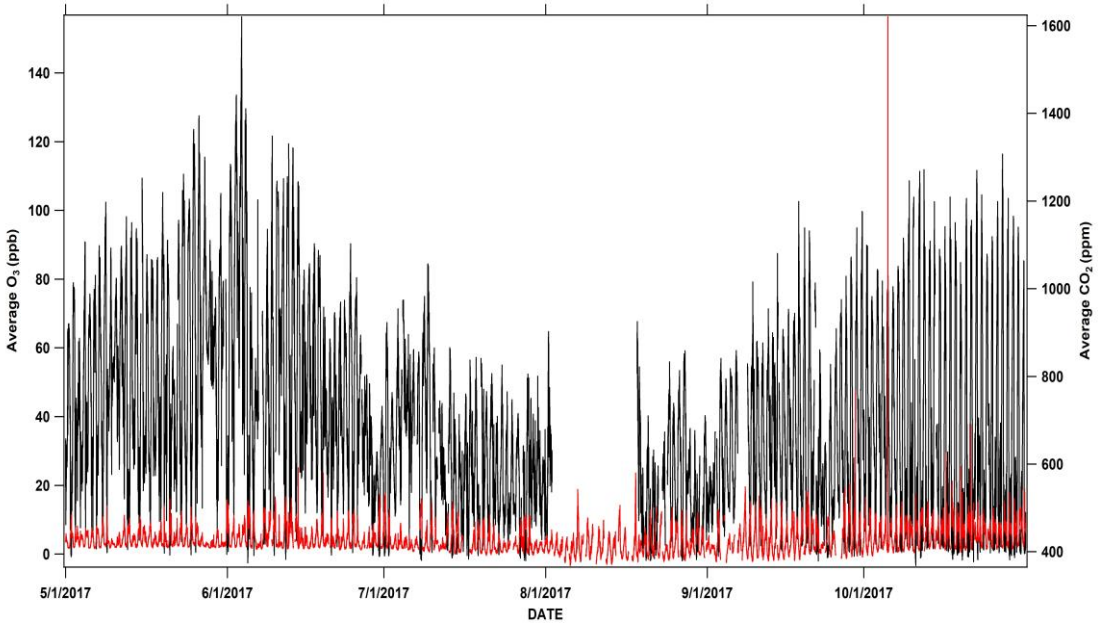

Figure 10: Average Ozone vs and CO_2 concentrations **(**Met-Data 2017) acquired from AQS sensor

emission sources like biogenic emission, paddy burning (a major problem in the region) etc. Ozone shows random ups and down during the observation period. Both trace gases play important role in plant-atmosphere chemistry as they both are dynamic in nature (can form compounds rapidly with each other). The mole fraction for each gas with respect to air defines the Ozone-CO_2 mixing ratio. This ultimately can affect the stomatal conductance of the plant as seen in our study.

3.2 Species-wise analysis of box plots and comparison

The box and whisker plot gives the relationship between stomatal conductance (g_{sto}) and hour of the day for all 5 tree species. The width of the box represents the interquartile range (25th and 75th percentiles), while the whiskers represent the 10th and 90th percentiles of the data. The dividing line in mid between the boxes, in each plot, shows the median while the average is shown as a black dot. The plots were made using IGOR Pro by Wavemetrics.

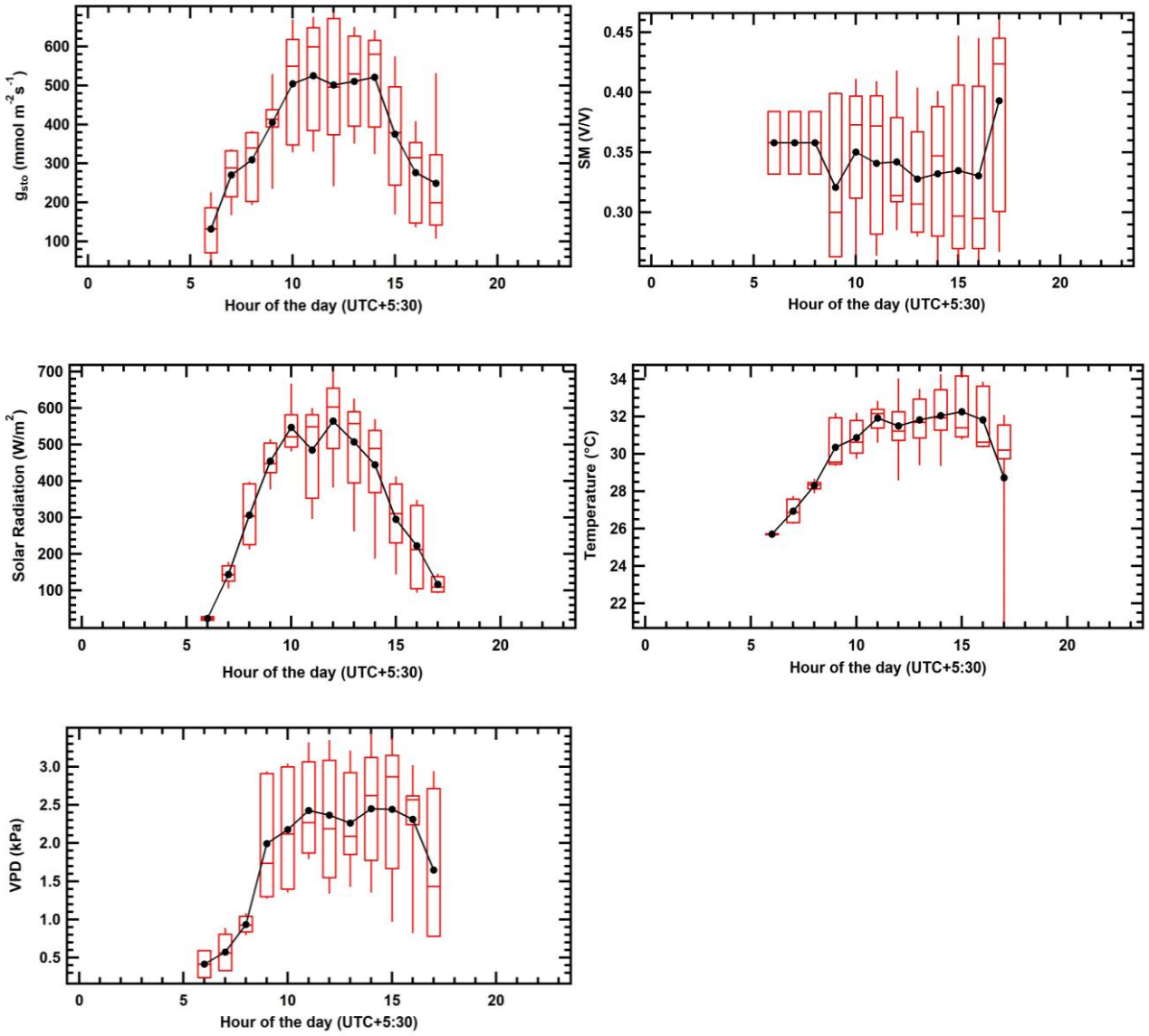

Figure 11: Box and whisker plots showing hourly average of g_{sto} (stomatal conductance), Soil moisture (V/V), Solar Radiation (W/m^2), Temperature (°C), VPD (kPa) for *C. fistula*

3.2.1 *Cassia fistula*

C. fistula are in a series plantation beside the common road in IISER Mohali. Only shade they get is from each other. Figure 11 shows the box and whisker plots, which comprised of hourly average data for g_{sto}, VPD, Air temperature, VPD, SM and Solar Radiation. The general trend is with increasing in temperature solar radiation, PAR and VPD increases. In the plot it is visible that sunrises around 7 a.m and temperature start increasing afterwards. VPD starts and solar radiation rapidly increases after 8 a.m onwards. On the other hand Soil moisture shows opposite trend i.e. it decreases as temperature starts increasing due to plant uptake of water through roots. The average stomatal conductance is 362 mmol $m^{-2}s^{-1}$.The stomatal conductance reach its peak around pre noon time and starts decline in the evening around 3 p.m which is similar to VPD plot. Hence drying power of air has effect on the stomata on this tree.

3.2.2 *V. nilotica*

V. nilotica is alone tree near the main road at IISER Mohali with no shade factor but wind and emission effects can be huge. Figure 12 shows box and whisker plots for *V. nilotica* tree. The average stomatal conductance is 253 mmol $m^{-2}s^{-1}$ .The box and whisker plots show the general trend. However around 11a.m, there are some dips in solar radiation as well as in stomatal conductance which could be due to cloud factor which is often seen during monsoon season.

3.2.3 *P. pinnata*

P. pinnata is facing maximum emission as it is most close to main road at IISER Mohali and receive shades from nearby trees of same species. Figure 13 shows box and whisker plots for *P. pinnata* tree. The average stomatal conductance is 245 mmol $m^{-2}s^{-1}$. The plots shows usual trends except at few early morning timings. Around 9-10a.m there are up and down peaks of stomatal conductance and solar radiation. Here these variation could be due to cloud factor as seen in monsoon or pre monsoon season.

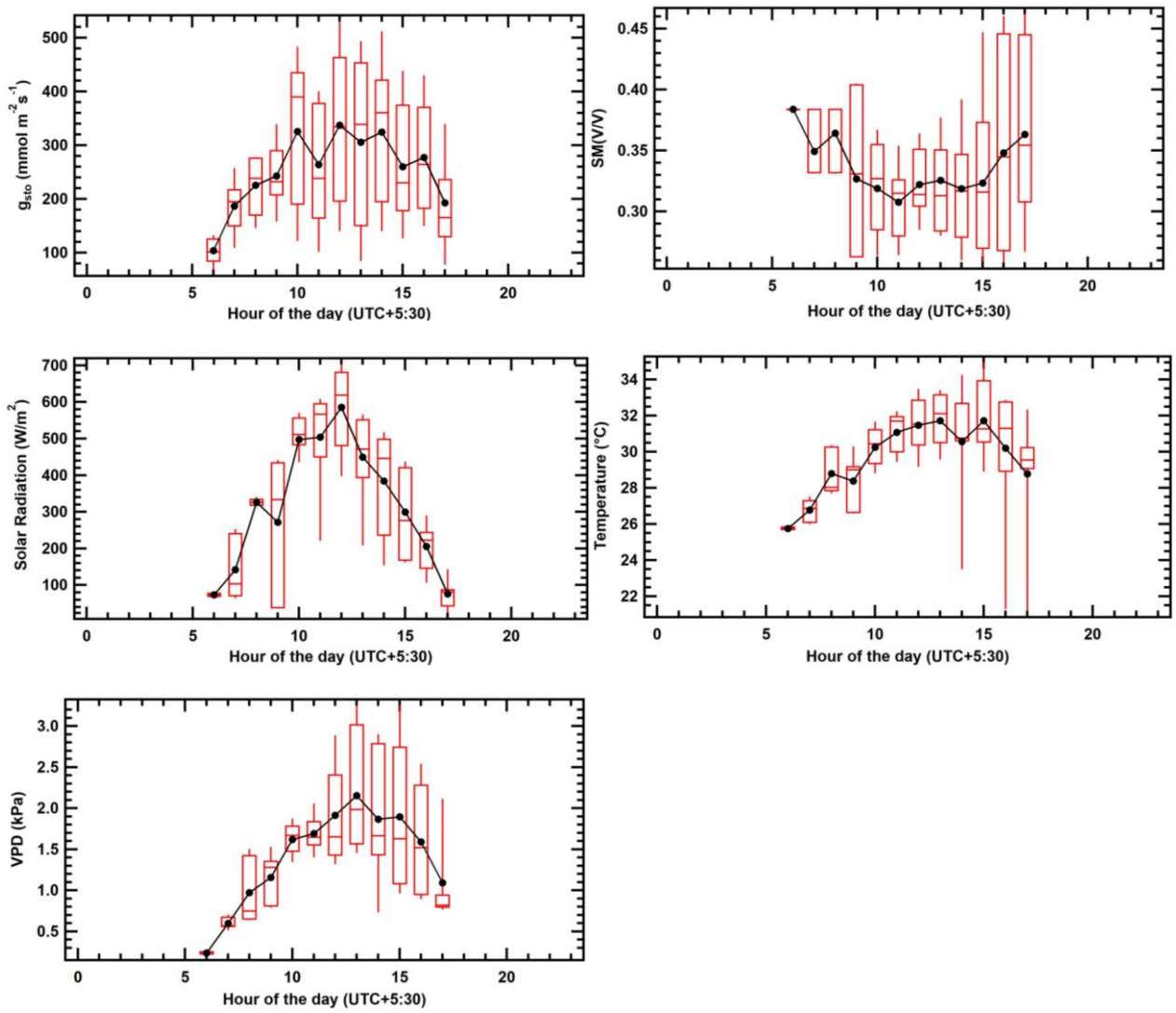

Figure 12: Box and whisker plots showing hourly average of g_{sto} (stomatal conductance), Soil moisture (V/V), Solar Radiation (W/m^2), Temperature (°C), VPD (kPa) for *V. nilotica*

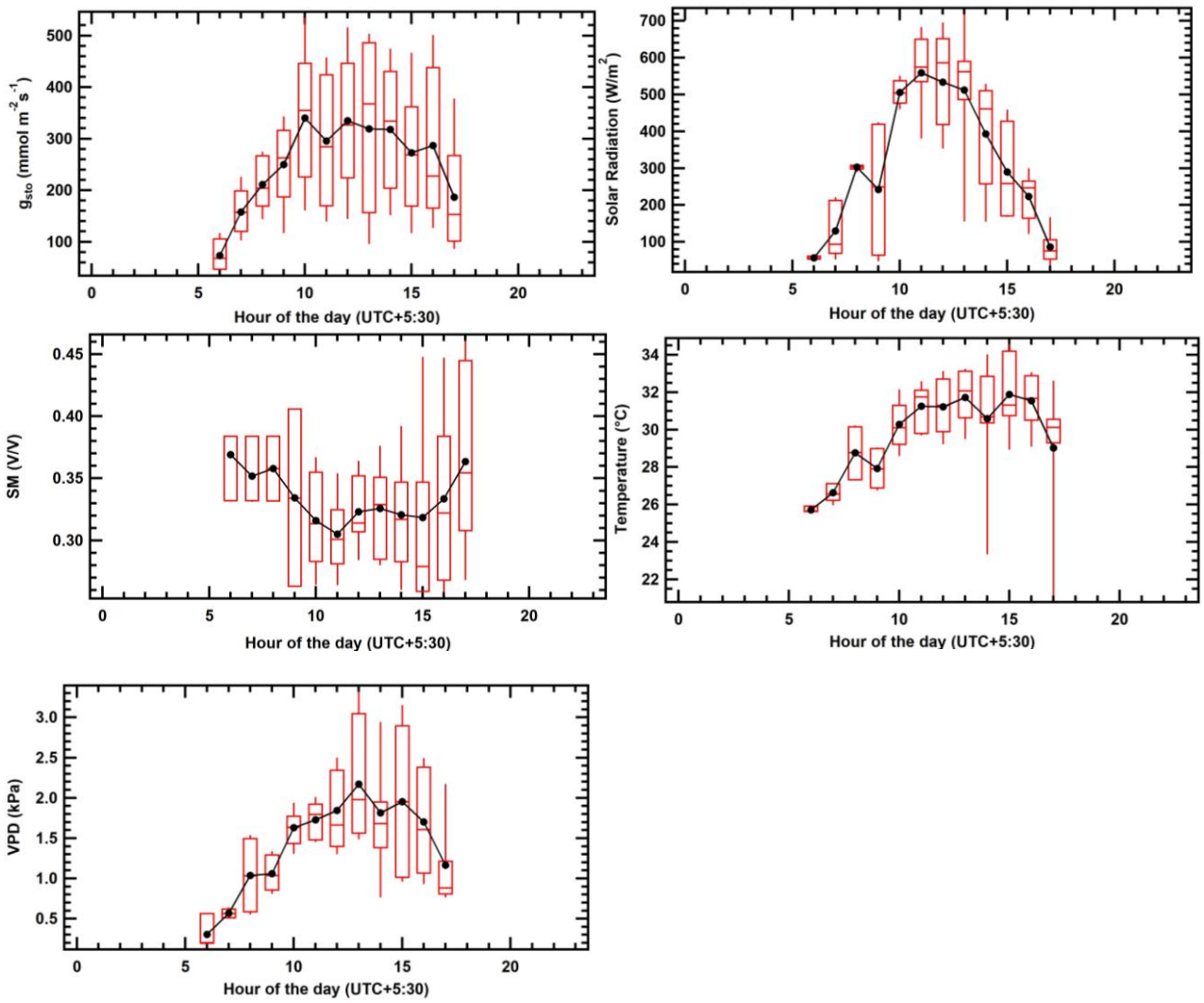

Figure 13: Box and whisker plots showing hourly average of g_{sto} (stomatal conductance), Soil moisture (V/V), Solar Radiation (W/m^2), Temperature (°C), VPD (kPa) for *P. pinnata*

3.2.4 *Ceiba speciosa*

C. speciosa is ornamental tree which has morphology and physiology similar to *Bombax ceiba*. As it is far from traffic road and surrounded by lush green trees and shrubs. It faces least effects of emissions. Shade factor could be limiting, as it face Canara Bank Building one side and on the other side tall Peepal (*Ficus religiosa*) tree stands, but it get enough sunlight for growth. Figure 14 shows box and whisker plots for C. *speciosa.* The average stomatal conductance observed is 270 mmol $m^{-2}s^{-1}$. The trends for different environmental parameters with respect to stomatal conductance shows usual trend. However at some point's stomatal conductance shows unusual behaviour with respect to temperature and solar radiation. The reason for this variable could be due to drying power of air as seen in the VPD plot steep rise in VPD factor. So VPD could be limiting factor but shade factor can't be ignored.

3.2.4 *D. sissoo*

D. sissoo is situated beside less traffic road and most far from vehicular emissions. Low level of wind and shade factor could limit the photosynthesis. Figure 15 shows box and whisker plots for *D. sissoo.* The average stomatal conductance is 295 mmol $m^{-2}s^{-1}$. The stomatal conductance show rapid rise in morning and stabilize near noon. The box plots shows general trend except near noon where VPD shows unusual behaviour. So the stabilized stomatal conductance could be due to variation in VPD. The limiting factor could be cloud too as temperature plots show average solar radiation increase with variation in VPD plot in noon time.

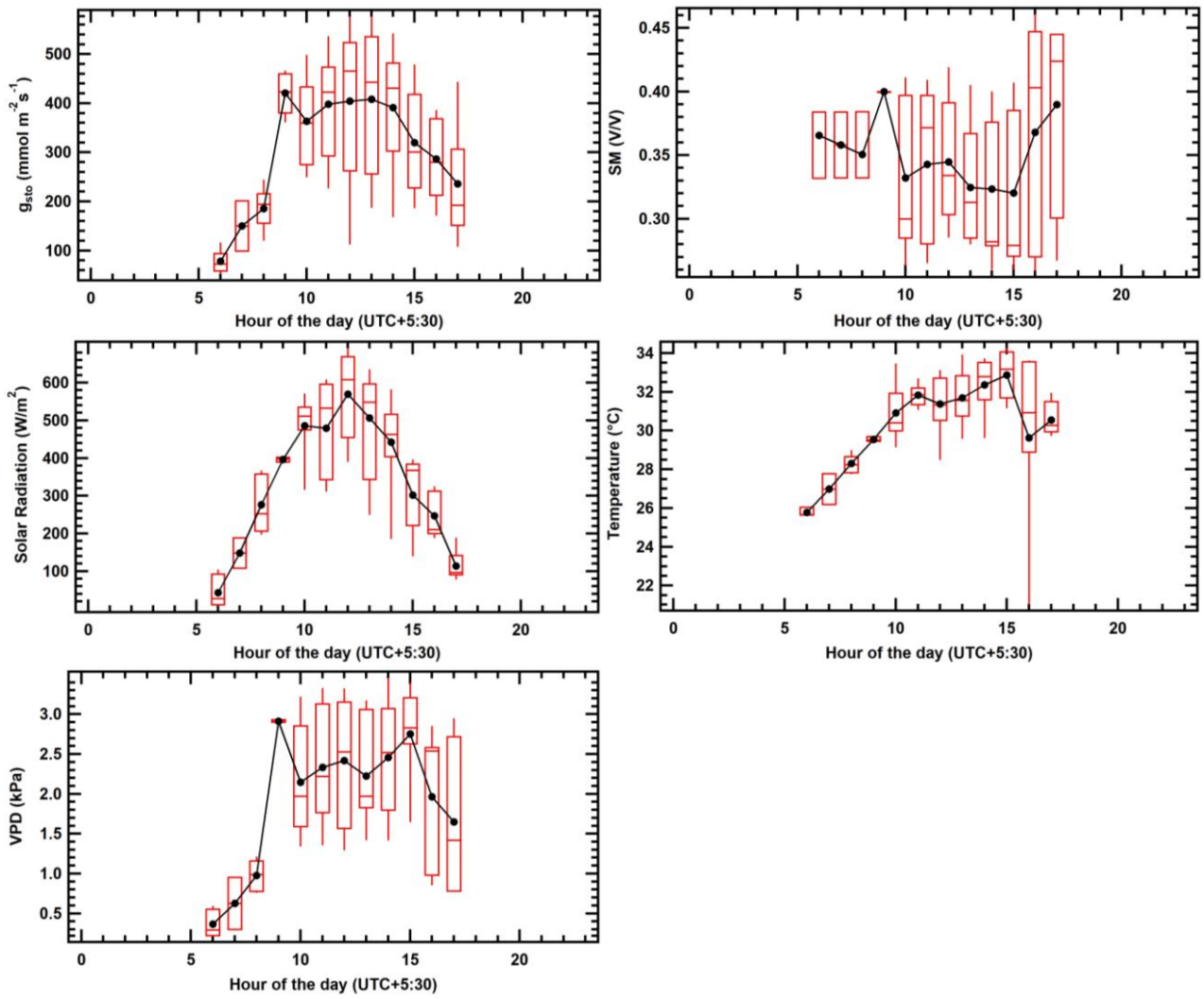

Figure 14: Box and whisker plots showing hourly average of g_{sto} (stomatal conductance), Soil moisture (V/V), Solar Radiation (W/m^2), Temperature (°C), VPD (kPa) for *C. speciosa*

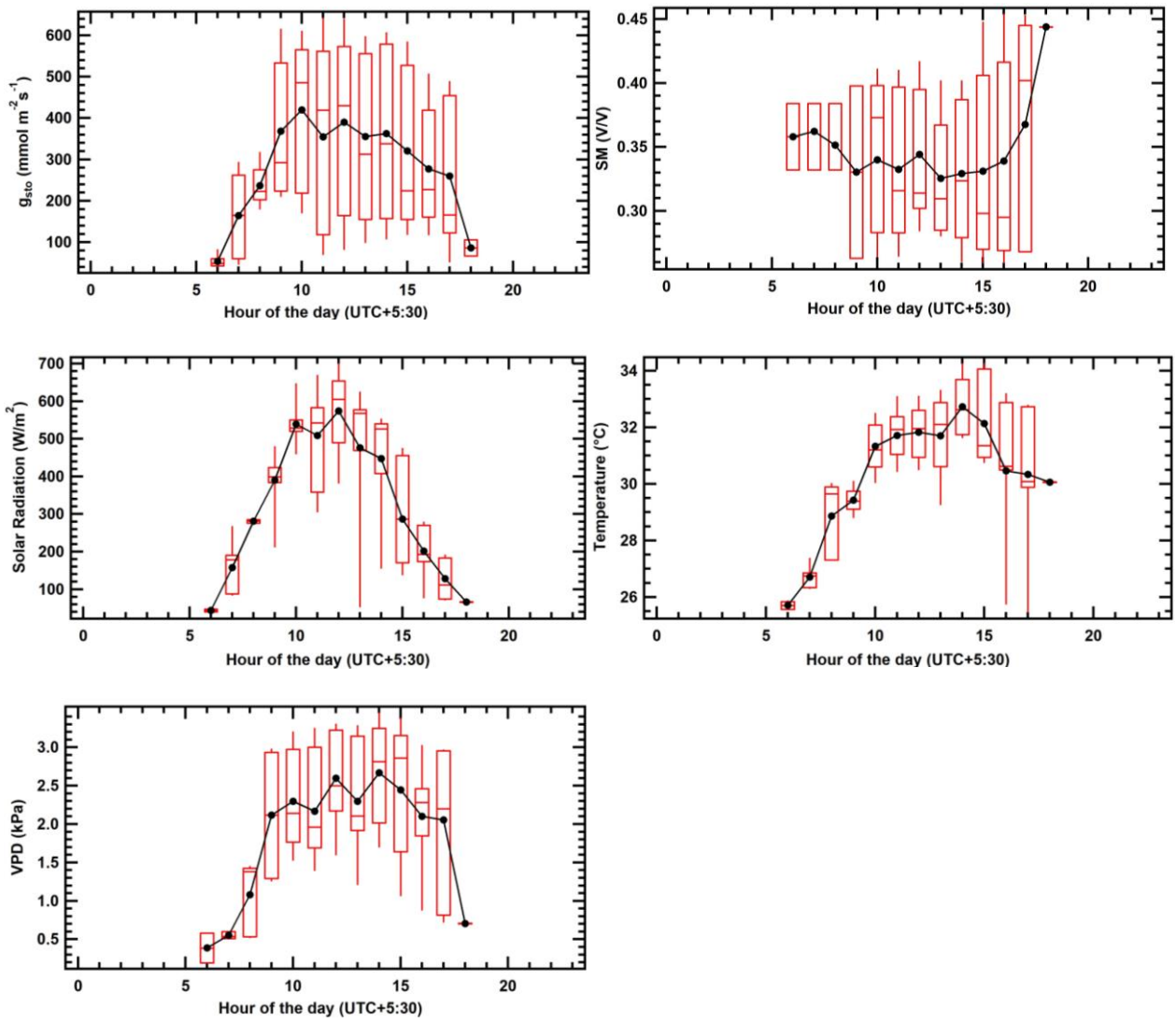

Figure 15: Box and whisker plots showing hourly average of g_{sto} (stomatal conductance), Soil moisture (V/V), Solar Radiation (W/m^2), Temperature (°C), VPD (kPa) for *D. sissoo*

3.3 Species-wise analysis of response functions and comparison

The stomatal conductance data obtained from field for each species, is used to derive response function for environmental factors and phenology. The plots are plotted between relative stomatal conductance and environmental factors. The response functions are calculated using standard formulations (Mills, 2017). Due to lack of phenology observations for tree, phenology function is not derived and interpreted based on literature. These response function will later help in deriving critical levels for Ozone for each studied trees. The response functions were plotted using MS-Excel.

3.3.1 *D. sissoo*

Figure 16 shows response functions for *D. sissoo.* The f_{light} function is given by alpha value (0.008) for the boundary line function in the plot. At low light level stomata rises rapidly and then stabilizes. This shows that stomata open early in response to PAR and PAR can be used for photosynthesis efficiently. The phenology plots shows that during June-July as new flowers appear and the stomatal uptake increases due to physiological demand. The f_{temp} gives the optimum temperature around 32°C, which shows tree is drought resistance and can tolerate heat stress. The air drying power is given by VPD function. The observed VPD_{max} and VPD_{min} were around 3.4 (kPa) and 5.3 (kPa) respectively. The stomata not only tolerates temperature (T_{max} = 45°C) but also stays open for high relative humidity. Soil moisture plays critical role as water stress can hinder normal physiological functions. The SM_{min} and SM_{max} were around 12% and 14% respectively. The low soil moisture content doesn't affect the stomata opening.

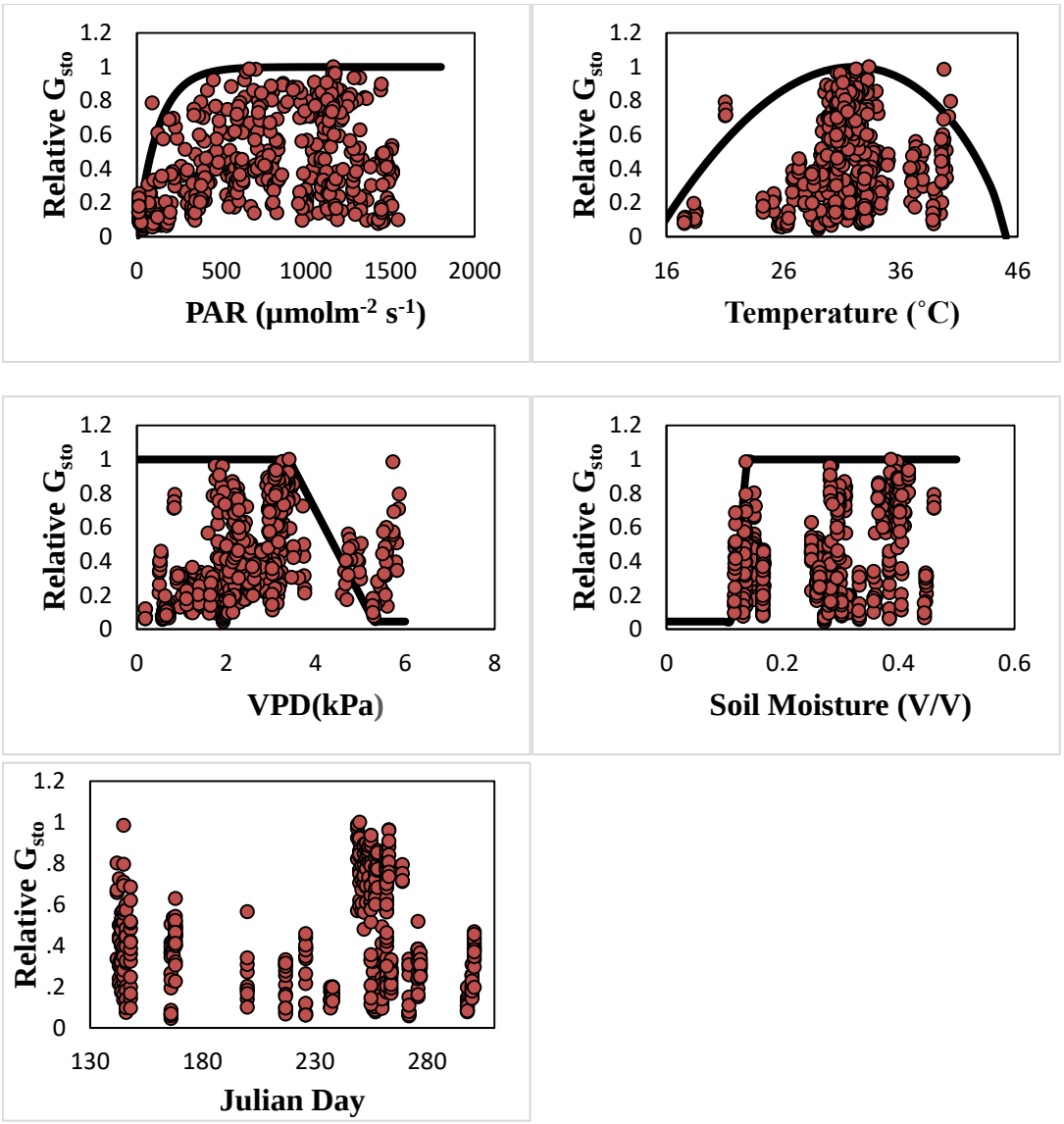

Figure 16: Plots of Relative G_{sto} vs PAR, Air temperature, VPD, SM and Phenology functions respectively for *D. sissoo*

3.3.2 *V. nilotica*

Figure 17 shows the response function for *V. nilotica*. The flowering and fruiting for the tree is highly regulated by temperature and rainfall. As the phenology function shows high stomata uptake after June onwards when fruiting and flowering occurs. The flight function gives alpha value around 0.009.Temperature function gives optimal temperature around 45°C which affirms the survivability of V. nilotica in diverse climatic conditions. T_{opt} is around 31°C, which shows it can efficiently do photosynthesis during the day. The VPD and Soil Moisture response functions shows similar trend as observed for other species.

3.3.3 *P. pinnata*

Figure 18 shows response functions plotted for *P. pinnata.* The phenology function shows high value for stomatal conductance near flowering and fruiting period. The Soil Moisture and VPD response function shows similar trend as shown by other species. The rapid rise in stomatal conductance at low light level shows leaf sensitivity towards PAR. The alpha value derived was around 0.0055. The optimal temperature was observed at 32°C and shows that stomata can tolerate heat and can work efficiently at high temperature.

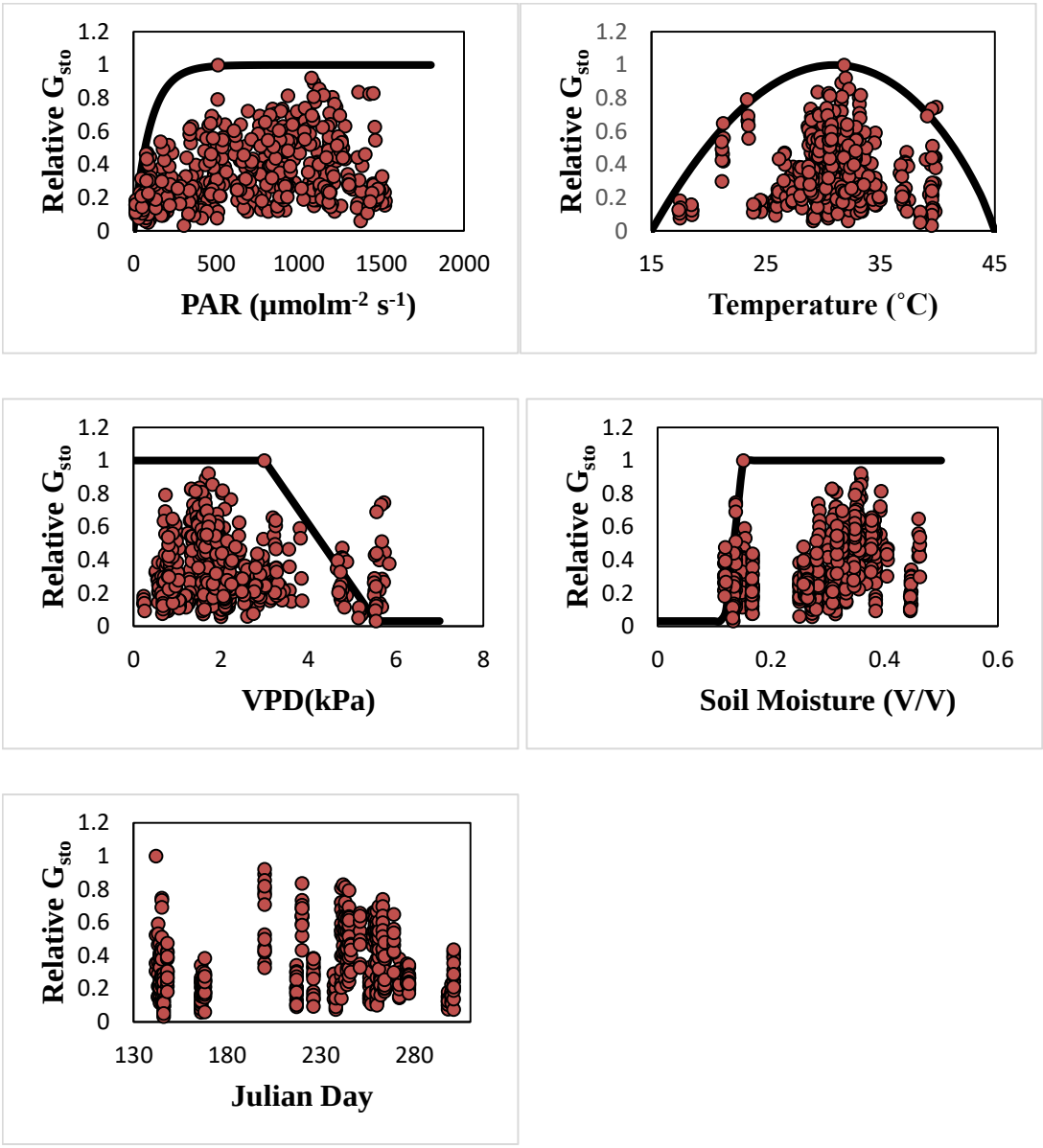

Figure 17: Plots of Relative G_{sto} vs PAR, Air temperature, VPD, SM and Phenology functions respectively for *V. nilotica*

3.3.4 *Cassia fistula*

The response function for *C. fistula* is shown in Figure 19. This tree species often received external watering so Soil Moisture function need to be carefully examined. The tree PAR response function gives alpha value of 0.0065 which shows it also opens its stomata in low light. The optimal temperature for stomatal uptake was found to be 32°C and hence it can tolerate high temperature too. This species show maximum stomatal conductance. The flowering period starts from May and can end it October. In the phenology response function, high physiological activity can be seen during May to July as new leaves emerges and flowering goes on. VPD function shows similar trend as observed for other species.

3.3.5 *Ceiba speciosa*

Figure 20 shows response function for C. speciosa. Similarly this tree species often received external watering near it, so Soil Moisture function need to be carefully examined. The phenology response function shows higher ozone uptake around post monsoon season as floral bud start to appearing. The VPD function shows similar trend as observed for other tree species. In the later stage yellowing of the leaf starts to appear which could be sign of late stage ozone damage as older leaves are unable to scavenge ozone efficiently and hence tissues die. The alpha value derived using light function was around 0.0055 which is similar to P. pinnata. The temperature function gives the optimal temperature around 30°C. The low G_{max} could be due to shade factor as it is in front of a building.

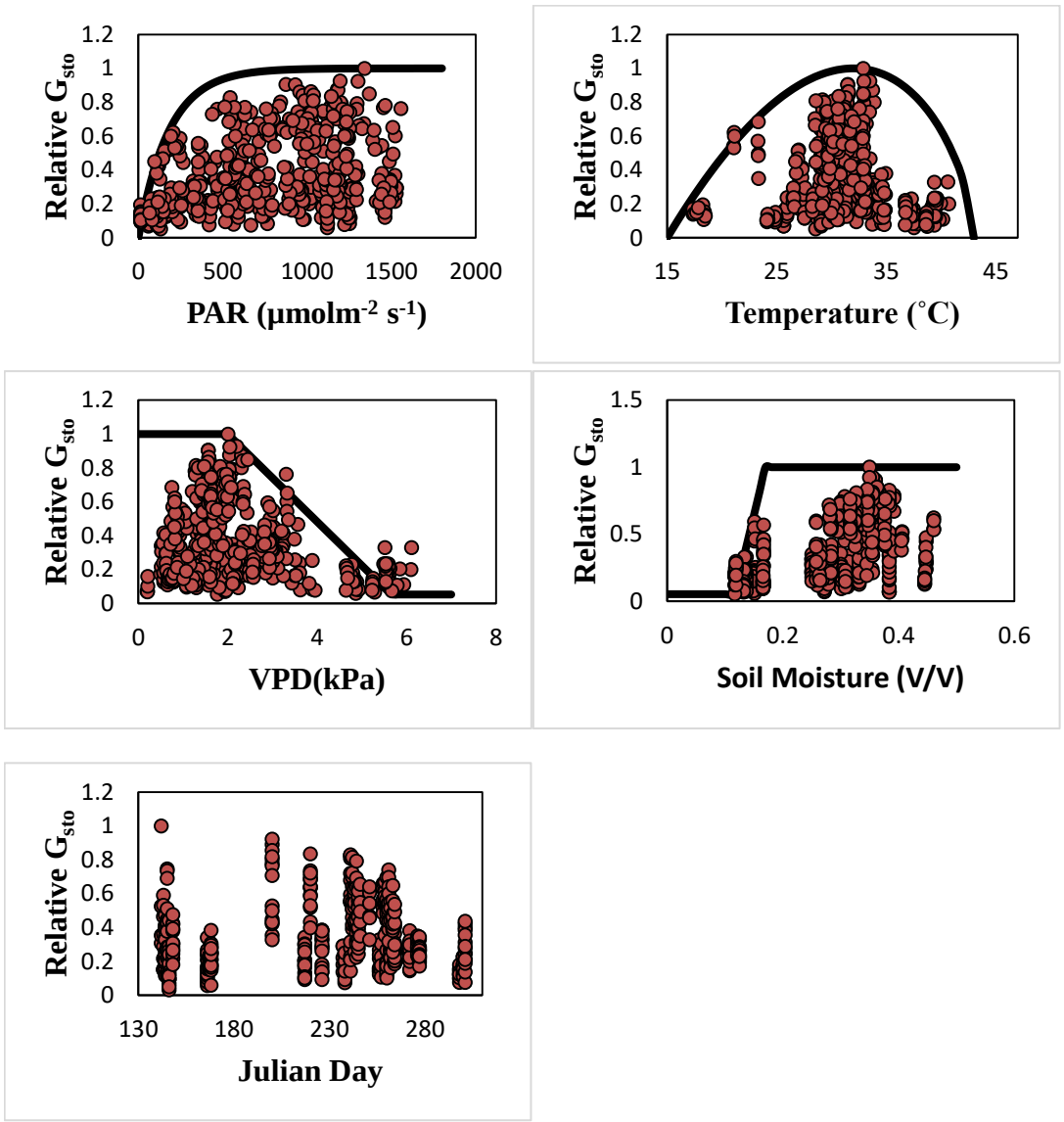

Figure 18: Plots of Relative G_{sto} vs PAR, Air temperature, VPD, SM and Phenology functions respectively for *P. pinnata*

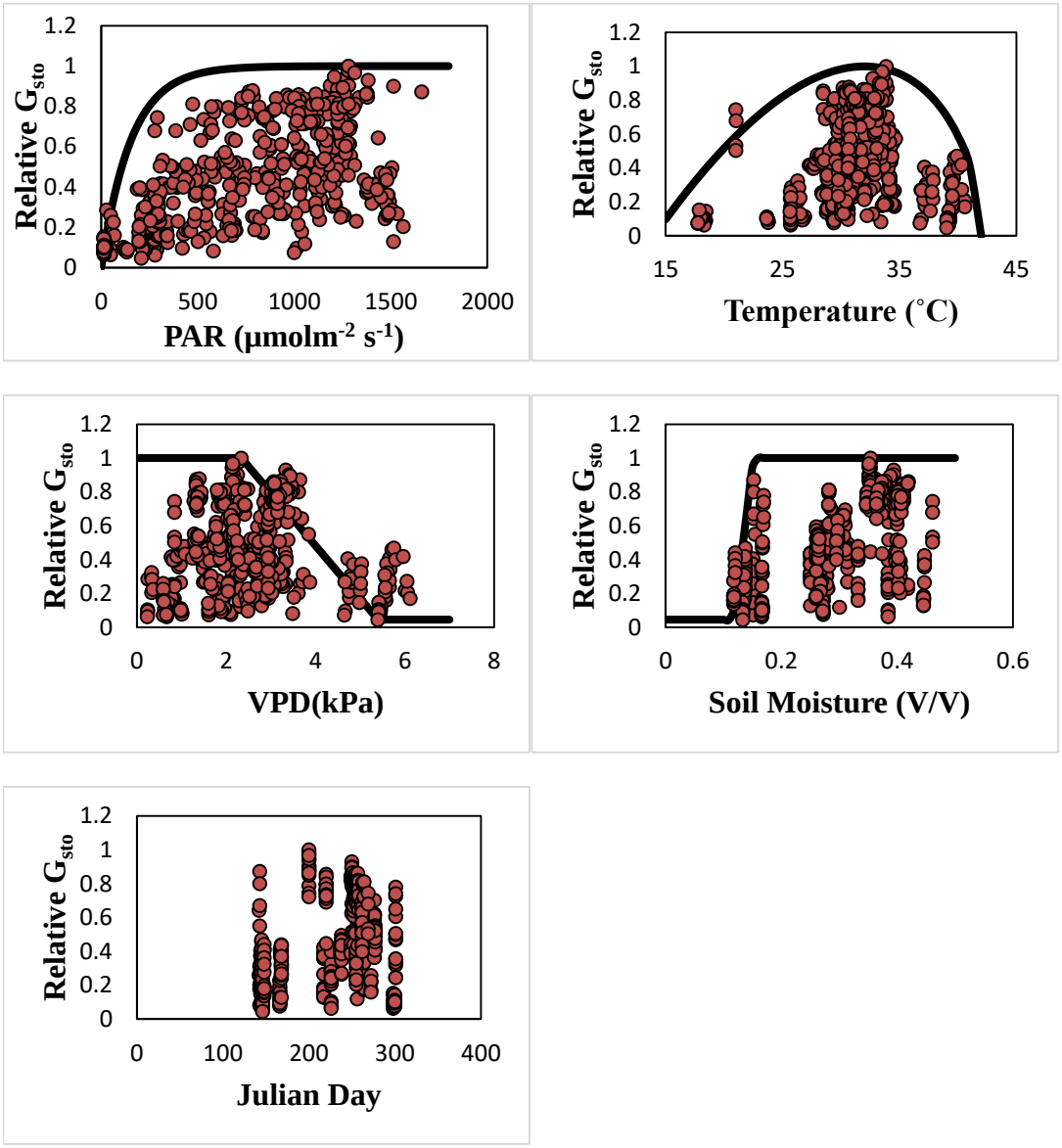

Figure 19 : Plots of Relative G_{sto} vs PAR, Air temperature, VPD, SM and Phenology functions respectively for *C. fistula*

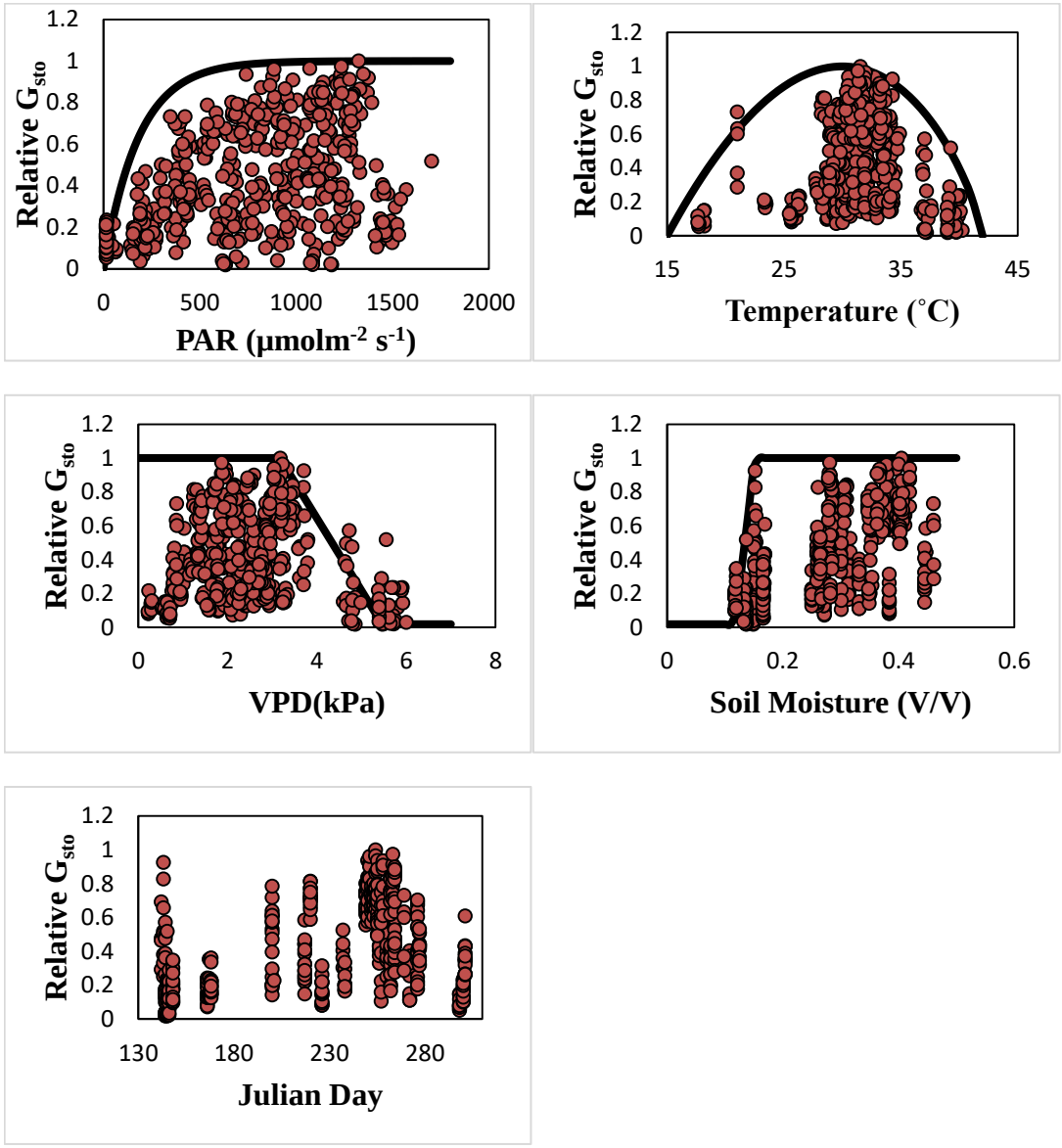

Figure 20 : Plots of Relative G_{sto} vs PAR, Air temperature, VPD, SM and Phenology functions respectively for *C. speciosa*

3.4 Parameterization Table

In Table 1, the parameterization of the DO3SE model for above studied 5 species is shown as a comparison to the parametrization done on Psidium guajava (Assis et al. 2015). India is one of the largest guava producing country and this study can be helpful in finding yield loss.

Since work done on P. guajava is from Brazil, a tropical country having almost similar climatic conditions and most parameters like f_{light}, f_{temp}, f_{vpd}, $f_{min,}$ and g_{max} shows similar trends except soil moisture, alpha value (f_{light}) and f_{vpd}. The reason for differences could be: the stomatal conductance data taken composed of Monsoon and post-monsoon season and tree species are situated at variable distances from each other as well as from soil moisture sensor (Decagon Sensor).

Parameters	***P guajava***	***D. sissoo***	***P. pinnata***	***V. nilotica***	***C. fistula***	***C. speciosa***
G_{max} (mmol/m^2s^1)	721	692.9	661.74	724.96	799.8	629.06
f_{min} (G_{min}/G_{max})	0.026	0.045	0.053	0.032	0.046	0.019
f_{light} (α)	0.014	0.008	0.0055	0.009	0.0065	0.0055
T_{min} (°C)	15	15	15	15	14	15
T_{opt} (°C)	28	32	32	31	32	30
T_{max} (°C)	43	45	43	45	42	42
VPD_{max} (kPa)	1.2	3.4	2.0	2.99	2.34	3.17
VPD_{min} (kPa)	5.5	5.3	5.66	5.54	5.4	5.46
SM_{max}	0.22	0.137	0.17	0.151	0.152	0.152
SM_{min}	0.03	0.117	0.117	0.118	0.117	0.117

Table 1: Comparison of g_{sto} parameterization between *P. guajava* and above studied tree species

3.5 Maximum Stomatal Conductance

Maximum Stomatal Conductance (G_{max}) gives an idea of stomatal flux capacity of a tree species and ozone uptake for a particular time period. Table 2 shows the maximum stomatal conductance for all five trees studied. Higher G_{max} is associated with higher photosynthesis and generally obtained when the tree is highly active physiologically and stomata are open maximally for gaseous exchange for a longer period of time. The G_{max} is obtained by converting g_{max} by a conversion factor of 0.663 because there is a difference in the molecular diffusivity of water vapor with respect to ozone (Massman et al.1998; Grünhage et al., 2012).

Tree species	G_{max} (mmol O_3 $m^{-2}s^{-1}$)
D. sissoo	459.3927
P. pinnata	438.73362
V. nilotica	480.64848
C. fistula	530.2674
C. speciosa	417.06678

Table 2 : Shows different trees studied and their respective G_{max} (Maximum Stomatal Conductance)

Chapter 4

Summary and Conclusion

Indo-Gangetic plains are considered most fertile land in India, recently there has been a rapid increment in vehicular emission, biogenic emission, combustion emission, industrial emission etc. These emissions comprised of precursor compounds for tropospheric ozone. In India, most of the ozone risk assessment and studies are done using the AOT40 metric, which is exposure based metric proposed by Fuhrer et al. (1997). However, the AOT40 metric can be employed in ex-situ or regulated conditions where nutrients, water, and other plant growth factors are optimal. In field conditions, the plant faces abiotic stress which also comprised of pollutant uptake by plants, this can be accounted for effectively using flux-based models like DO3SE model (Karlsson et al. 2007). Moreover, there has been no published study in India which has shown any parameterization of ozone risk assessment models for trees.

In this study, we did the parameterization of the DO3SE model for five tree species and concluded that model can be applied to the studied five tree species. This kind of the study in these tree species is done for the first time. But the accuracy of the parameterization can be improved if we take more observation under varying climatic conditions at more places for the same tree species. More functions can be incorporated in the model for better accuracy.

Although there are studies where an ozone risk assessment has been done on trees using DO3SE model and model performance was check. (Alonso et al., 2008; Kinose et al., 2014)

However, above-mentioned studies are different our studies as they were done using open-top chamber or O_3 fumigation closed chamber.

In contrast, some researchers say that current ozone risk models, based on European and North American data, provide inaccurate estimates for crop losses in India (Oksanen et al., 2013).

DO3SE model can be the answer to the shortcomings of the current assessment model used in India (AOT40), as it has been improved with continuous studies. In India, it is necessary to set the critical level for ozone-induced effects to vegetation, as our country is an agrarian economy and crop yield loss need to be prevented. Moreover, vegetation needs to be protected from ozone-induced effects caused by air pollution and increasing radiative forcing. More diverse studies are needed to find the solution for the increasing toxic effects of tropospheric ozone.

Bibliography

Alonso, R., Elvira, S., Sanz, M. J., Gerosa, G., Emberson, L. D., Bermejo, V., & Gimeno, B. S. (2008). Sensitivity analysis of a parameterization of the stomatal component of the DO3SE model for Quercus ilex to estimate ozone fluxes. *Environmental Pollution*, *155*(3), 473–480. https://doi.org/10.1016/j.envpol.2008.01.032

Alvarado R., D., de Bauer, L. I., & Galindo A., J. (1993). Decline of sacred fir (Abies religiosa) in a forest park south of Mexico City. *Environmental Pollution*. https://doi.org/10.1016/0269-7491(93)90136-C

Ashmore, M. R. (2005). Assessing the future global impacts of ozone on vegetation. *Plant, Cell and Environment*. https://doi.org/10.1111/j.1365-3040.2005.01341.x

Assis, P. I. L. S., Alonso, R., Meirelles, S. T., & Moraes, R. M. (2015). DO3SE model applicability and O3flux performance compared to AOT40 for an O3-sensitive tropical tree species (Psidium guajava L. 'Paluma'). *Environmental Science and Pollution Research*, *22*(14), 10873–10881. https://doi.org/10.1007/s11356-015-4293-1

Atkinson, R. (2000). Atmospheric chemistry of VOCs and NO(x). *Atmospheric Environment*. https://doi.org/10.1016/S1352-2310(99)00460-4

Büker, P., Morrissey, T., Briolat, A., Falk, R., Simpson, D., Tuovinen, J. P., … Emberson, L. D. (2012). DO3SE modelling of soil moisture to determine ozone flux to forest trees. *Atmospheric Chemistry and Physics*, *12*(12), 5537–5562. https://doi.org/10.5194/acp-12-5537-2012

Chaudhary, I. J., & Rathore, D. (2018). Suspended particulate matter deposition and its impact on urban trees. *Atmospheric Pollution Research*. https://doi.org/10.1016/j.apr.2018.04.006

Devices, D. (2016). *Operator's Manual Decagon Devices, Inc*. Retrieved from www.decagon.com

Emberson, L. D., Ashmore, M. R., Cambridge, H. M., Simpson, D., & Tuovinen, J. P.

(2000). Modelling stomatal ozone flux across Europe. In *Environmental Pollution* (Vol. 109, pp. 403–413). https://doi.org/10.1016/S0269-7491(00)00043-9

Emberson, L. D., Kitwiroon, N., Beevers, S., Büker, P., & Cinderby, S. (2013). Scorched earth: How will changes in the strength of the vegetation sink to ozone deposition affect human health and ecosystems? *Atmospheric Chemistry and Physics*. https://doi.org/10.5194/acp-13-6741-2013

Fowler, D., Pilegaard, K., Sutton, M. A., Ambus, P., Raivonen, M., Duyzer, J., … Erisman, J. W. (2009). Atmospheric composition change: Ecosystems-Atmosphere interactions. *Atmospheric Environment*. https://doi.org/10.1016/j.atmosenv.2009.07.068

González-Fernández, I., Bermejo, V., Elvira, S., Sanz, J., Gimeno, B. S., & Alonso, R. (2010). Modelling annual pasture dynamics: Application to stomatal ozone deposition. *Atmospheric Environment*. https://doi.org/10.1016/j.atmosenv.2010.04.033

Grünhage, L., Pleijel, H., Mills, G., Bender, J., Danielsson, H., Lehmann, Y., … Bethenod, O. (2012). Updated stomatal flux and flux-effect models for wheat for quantifying effects of ozone on grain yield, grain mass and protein yield. In *Environmental Pollution*. https://doi.org/10.1016/j.envpol.2012.02.026

GUNDERSON, C. A., & TAYLOR, G. E. (1988). Kinetics of inhibition of foliar gas exchange by exogenous ethylene: an ultrasensitive response. *New Phytologist*. https://doi.org/10.1111/j.1469-8137.1988.tb00291.x

Hauglustaine, D. A., Brasseur, G. P., Walters, S., Rasch, P. J., Müller, J. F., Emmons, L. K., & Carroll, M. A. (1998). MOZART, a global chemical transport model for ozone and related chemical tracers 2. Model results and evaluation. *Journal of Geophysical Research Atmospheres*. https://doi.org/10.1029/98JD02398

Hofstra, G., Ali, A., Wukasch, R. T., & Fletcher, R. A. (1981). The rapid inhibition of root respiration after exposure of bean (Phaseolus vulgaris L.) plants to ozone. *Atmospheric Environment (1967)*. https://doi.org/10.1016/0004-6981(81)90178-5

Hoshika, Y., Carriero, G., Feng, Z., Zhang, Y., & Paoletti, E. (2014). Determinants of stomatal sluggishness in ozone-exposed deciduous tree species. *Science of the Total*

Environment, *481*(1), 453–458. https://doi.org/10.1016/j.scitotenv.2014.02.080

Jacob, D. J. (2000). Heterogeneous chemistry and tropospheric ozone. *Atmospheric Environment*. https://doi.org/10.1016/S1352-2310(99)00462-8

Jarvis, P. G. (1976). The Interpretation of the Variations in Leaf Water Potential and Stomatal Conductance Found in Canopies in the Field. *Philosophical Transactions of the Royal Society B: Biological Sciences*. https://doi.org/10.1098/rstb.1976.0035

Karnosky, D. F., Pregitzer, K. S., Zak, D. R., Kubiske, M. E., Hendrey, G. R., Weinstein, D., … Percy, K. E. (2005). Scaling ozone responses of forest trees to the ecosystem level in a changing climate. *Plant, Cell and Environment*. https://doi.org/10.1111/j.1365-3040.2005.01362.x

Kinose, Y., Azuchi, F., Uehara, Y., Kanomata, T., Kobayashi, A., Yamaguchi, M., & Izuta, T. (2014). Modeling of stomatal conductance to estimate stomatal ozone uptake by Fagus crenata, Quercus serrata, Quercus mongolica var. crispula and Betula platyphylla. *Environmental Pollution*. https://doi.org/10.1016/j.envpol.2014.07.030

Kulkarni, P. S., Ghude, S. D., & Bortoli, D. (2010). Tropospheric ozone (TOR) trend over three major inland Indian cities: Delhi, Hyderabad and Bangalore. *Annales Geophysicae*, *28*(10), 1879–1885. https://doi.org/10.5194/angeo-28-1879-2010

Massman, W. J. (1998). A review of the molecular diffusivities of H2O, CO2, CH4, CO, O3, SO2, NH3, N2O, NO, and NO2in air, O2and N2near STP. *Atmospheric Environment*. https://doi.org/10.1016/S1352-2310(97)00391-9

Mills, G. (2017). Mapping Critical Levels for Vegetation. In *Manual on Methodologies and Criteria for Modelling and Mapping Critical Loads and Levels and Air Pollution Effects, Risks and Trends.*

Mills, G., Pleijel, H., Braun, S., Büker, P., Bermejo, V., Calvo, E., … Simpson, D. (2011). New stomatal flux-based critical levels for ozone effects on vegetation. *Atmospheric Environment*. https://doi.org/10.1016/j.atmosenv.2011.06.009

Oksanen, E., Pandey, V., Pandey, A. K., Keski-Saari, S., Kontunen-Soppela, S., & Sharma, C. (2013). Impacts of increasing ozone on Indian plants. *Environmental*

Pollution. https://doi.org/10.1016/j.envpol.2013.02.010

Padhy, P. K., & Varshney, C. K. (2005). Isoprene emission from tropical tree species. *Environmental Pollution*, *135*(1), 101–109. https://doi.org/10.1016/J.ENVPOL.2004.10.003

PUNJAB STATE ACTION PLAN Non-Conventional Energy Govt . of Punjab PUNJAB Draft Report December 2012. (2012), (December).

Saxena, P., & Ghosh, C. (2015). Seasonal variation of isoprene emissions from tropical roadside plant species and their possible role in deteoriating air quality, *4*(2), 67–80.

Schmidt, U., Thöni, H., & Kaupenjohann, M. (2000). Using a boundary line approach to analyze N2O flux data from agricultural soils. *Nutrient Cycling in Agroecosystems*. https://doi.org/10.1023/A:1009854220769

Sharkey, T. D., & Singsaas, E. L. (1995). Why plants emit isoprene [1]. *Nature*. https://doi.org/10.1038/374769a0

Shindell, D., Kuylenstierna, J. C. I., Vignati, E., Van Dingenen, R., Amann, M., Klimont, Z., … Fowler, D. (2012). Simultaneously mitigating near-term climate change and improving human health and food security. *Science*. https://doi.org/10.1126/science.1210026

Singh, R., & Singh, M. P. (2017). Volatile Organic Compounds (VOC) Emission from plant species of the Vidarbha, *2*(9), 12–16.

Sitch, S., Cox, P. M., Collins, W. J., & Huntingford, C. (2007). Indirect radiative forcing of climate change through ozone effects on the land-carbon sink. *Nature*. https://doi.org/10.1038/nature06059

Varshney, C. K., & Singh, A. P. (2003). Isoprene emission from Indian trees. *Journal of Geophysical Research: Atmospheres*, *108*(D24), n/a-n/a. https://doi.org/10.1029/2003JD003866

Whitehead, D., Barbour, M. M., Griffin, K. L., Turnbull, M. H., & Tissue, D. T. (2011). Effects of leaf age and tree size on stomatal and mesophyll limitations to photosynthesis in mountain beech (Nothofagus solandrii var. cliffortiodes). *Tree Physiology*. https://doi.org/10.1093/treephys/tpr021